DESIGN AND DEVELOPMENT OF SoC ESTIMATION MODEL USING MACHINE LEARNING

Project report submitted to
Visvesvaraya National Institute of Technology, Nagpur in partial fulfillment of the requirements for the award of the degree

BACHELOR OF TECHNOLOGY

IN

ELECTRICAL AND ELECTRONICS ENGINEERING

by

Abhigyan Chatterjee	**BT17EEE001**
Ansheel Banthia	**BT17EEE013**
Divyanshu Mehta	**BT17EEE026**
M.V.R.Subhash	**BT17EEE048**

under the guidance of

Dr. Krishnama Raju Suraparaju

Department of Electrical and Electronics Engineering

Visvesvaraya National Institute of Technology

Nagpur 440 010 (India)

2021

ABSTRACT

Living in the automation age and use of electric vehicles are becoming more common with every incoming day the proper utilization and estimation of the state of charge is very much required.

An accurate and fast estimation of state of charge of a battery will improve its efficiency and hence projects a clear picture to the customer when to charge and the most optimal journey will be possible.

We come with this motive to suggest and implement the data driven approach of calculation of the state of charge and use the state-of-the-art machine learning algorithms to find a solution to the problem as the traditional algorithms had a long processing time to evaluate the state of charge and were also computationally heavy.

List of Figures

List of Tables

Nomenclature

AC	Alternating Current
Ah	Ampere hour
A	Ampere
V	Volt
ICE	Internal Combustion Engine
SoC	State of Charge
DoD	Depth of Discharge
EFK	Extended Kalman Filter
FNN	Feed-forward Neural Network
DNN	Deep Neural Network
CNN	Convolutional Neural Network
LSTM	Long-short term memory
SVM	Support Vector Machine
ANN	Artificial Neural Network
RF	Random Forest
RMSE	Root mean square error
PNGV	Partnership for a New Generation of Vehicles.
PI	Proportional Integrator

Index

CHAPTER I

Introduction

Energy storage emerged as a top concern for the modern cities, and the choice of the lithium-ion battery as an effective solution for storage applications is proved to be highly efficient. Many electric vehicles have as a result started using Li-Ion batteries as the source of electrical energy. Hence, we need to now estimate SoC to optimize the performance and increase the lifetime of the Li-Ion battery.

1.1 Objectives of Our Project

- Literature Survey where we study the current domain challenges and various ML algorithms.
- We start Data Collection to train our model.
- Experiment with various ML algorithms to find the most optimized and efficient solution.
- Optimizing algorithm using various data interpretation and efficiency enhancement techniques.

1.2 Current Techniques for SoC Estimation

- Direct Measurements
    - Open Circuit Voltage (OCV)
    - Kalman Filter
    - Coulomb Counting Method
- Machine Learning model-based solution for SoC estimation.

CHAPTER II

BATTERY

2.1 Introduction

The word battery comes from the old French word “batteries” which means “action of beating”, relating to a group of cannons in battle. A battery is an energy storage device that represents multiple electrochemical cells connected together.

The battery is a feeble vessel that is slow to charge, holds limited energy, runs for a particular time and eventually runs out of charge.

The battery consists of two electrodes that are isolated by a separator and immersed in an electrolyte which helps in the movement of ions. When a battery is supplying electric power, it means that the electrons on the cathode reach the anode through an external circuit. There are two types of batteries:

1. Primary batteries- They are discarded once used as the electrode materials are irreversibly changed. Ex:-Alkaline batteries.
2. Secondary batteries-They can be charged and discharged multiple times using an applied current. Ex:-Lead-acid batteries.

Batteries have lower specific energy than common fuels like gasoline which becomes a bottleneck in the adoption of electric vehicles.

Batteries come in different shapes and sizes like the miniature cells used in wristwatches, thin cells used in mobiles and large batteries like lithium-ion used in electric vehicles.

Figure 2.1: Types of batteries

2.2 Working of a battery

An electrochemical battery consists of an anode, cathode and an electrolyte that allows the movement of ions. During charging positive ions buildup at the cathode electrolyte interface. This makes the electrons move towards the cathode from the anode creating a voltage potential between the electrodes. Release is by a passing current from the positive cathode through an external load and back to the negative anode.

A battery has two separate pathways: one is the electric circuit through which the electrons flow, feeding the load and the other path is through the electrolyte where ions move.

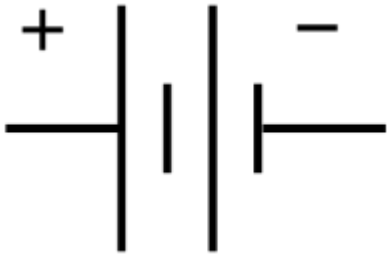

Figure 2.2: Symbol of a battery

2.3 Parameters of a battery

2.3.1 Energy storage

Batteries store energy reasonably well and for a long time. Primary batteries which are non-rechargeable hold more energy than secondary batteries which are to be recharged once emptied. This suggests that primary batteries have higher specific energy than secondary batteries. Also, the self-discharge is lower in primary batteries than that of secondary batteries.

2.3.2 Specific energy(capacity)

Compared to fossil fuels batteries have a lower specific energy. This implies that batteries can store a smaller amount of energy per unit mass than fossil fuels. The specific energy of gasoline is 12,000Wh/kg whereas the specific energy of a modern Li-ion battery is 200Wh/kg. However, a battery delivers energy more effectively than a thermal engine.

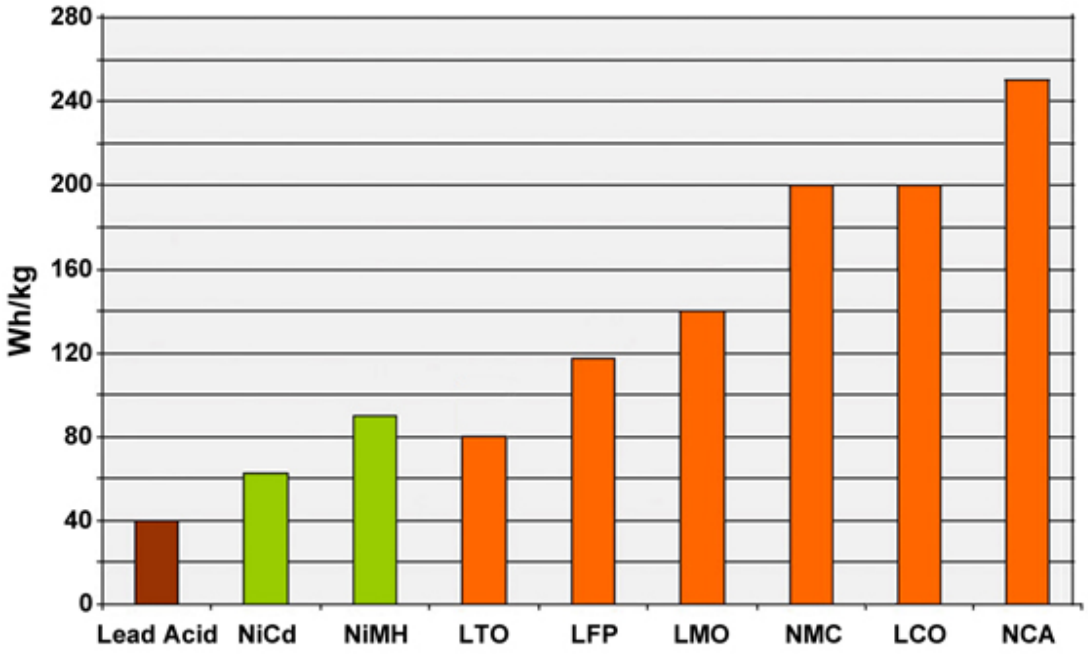

Figure 2.3: Typical specific energy of lead, nickel and lithium-based batteries

2.3.3 Responsiveness

In this case, the batteries have an advantage over other power sources because batteries can deliver power instantly whenever required. There are no conditions like warming up as in the case of an internal combustion engine (ICE) and due to this energy is delivered in a fraction of a second.

2.3.4 Power Bandwidth

Most rechargeable batteries have higher power bandwidth which means that they can handle a large variety of loads effectively. This gives batteries an upper hand and makes it suitable for a lot of applications.

2.3.5 Efficiency

The battery is highly efficient. Li-ion batteries have 99% charge efficiency and the discharge loss is small whereas the efficiency of ICE engines is about 25%-30%. This advantage slightly compensates for the lower specific energy of the battery compared to other power sources.

2.3.6 Service life:

The rechargeable battery has a service life of 3-5 years whereas the batteries used in electric vehicles are guaranteed to have a service life of 8-10 years. Large stationary batteries are good for 5-20 years.

2.3.7 Charge time

The biggest problem faced by the batteries can be seen over here. Lithium-based systems take about 1-3 hours to charge whereas filling the tank of the combustion engine hardly takes a few minutes. Temperature also plays a major role in charging and discharging time. At intense hot and cold conditions, the charge acceptance rate of a battery is low. So, it optimal to bring the te.

2.3.8 C rate

The C rate gives the measure at which a battery is being discharged or charged, It is the ratio of current through the battery to the theoretical current draw under which the battery would deliver its nominal rated capacity in one hour. Its units are h^{-1}.

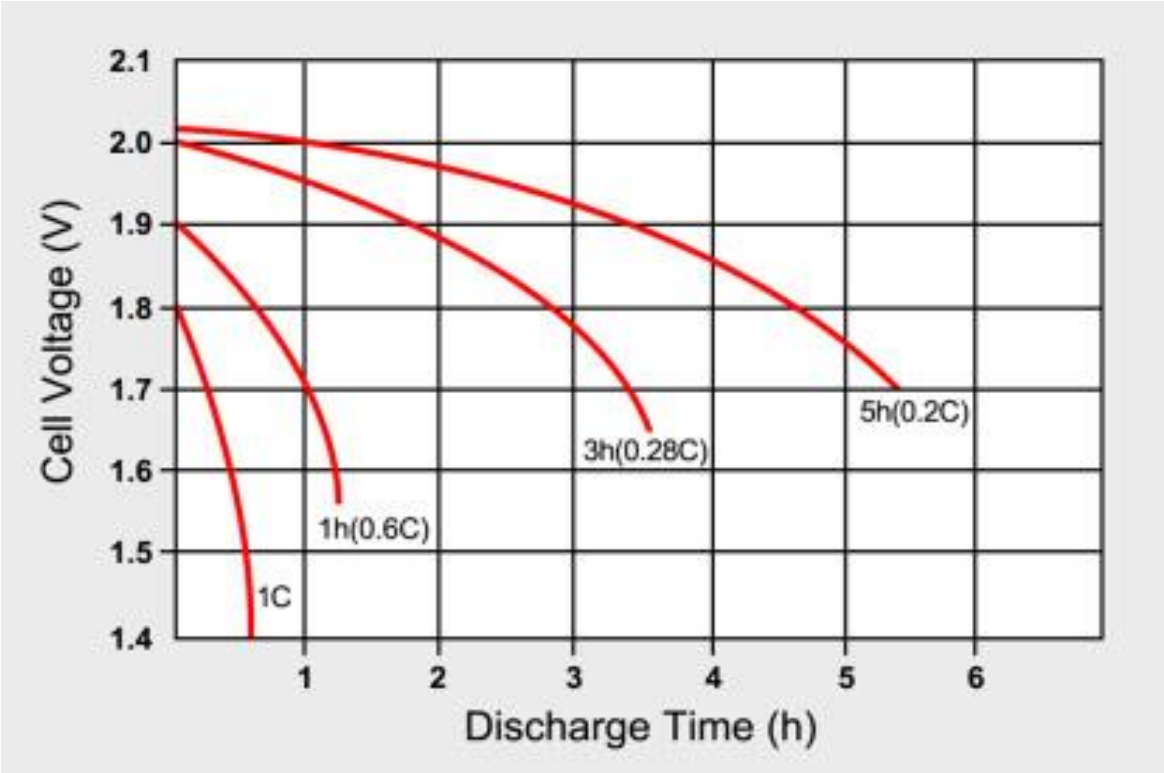

Figure 2.4: Typical discharge curves of lead-acid battery as a function of C-rate

2.3.9 Specific power

Specific power determines the loading capacity of a battery. Batteries made for power tools have specific power but come with reduced specific energy. This suggests that for a higher capacity of battery specific power must be below.

2.4 Lead-acid battery

Invented by French physician Gaston Plante in 1859, the lead-acid battery is the first rechargeable battery put into commercial use. The reasons that drove its commercial production are lead-acid is dependable and inexpensive at a cost.

The grid structure of a lead-acid battery is made out of lead alloy. Pure lead is soft and doesn't support itself, so small quantities of other metals are mixed to give mechanical strength and improve electrical properties. Some common additives are antimony, selenium and tin.

Lead-acid batteries are heavy and less durable than nickel and lithium-based batteries. A full discharge causes strain and with every discharge or charge cycle, the capacity of the battery slowly fades away. This wear down characteristic occurs in all batteries but in various degrees. A typical lead-acid battery provides about 200-300 discharge/charge cycles. The main reason for it,s relatively short life cycle are grid corrosion on the positive electrode, expansion of the positive plates and depletion of the active material. This ageing phenomenon is elevated at higher temperatures and also when a high discharge current is drawn.

Charging a lead-acid battery is simple but the correct voltage limits must be observed. Choosing a low voltage limit shelters the battery, but this causes poor performance and a build-up of sulfation on the negative plate. On the other hand, a high voltage limit improves performance but causes grid corrosion. Lead-acid batteries take about 14-16 hours to charge completely.

Even though at a whopping 99% recyclable rate the lead-acid batteries are being replaced by Lithium-ion batteries because lead is toxic and poses an environmental hazard.

Table 2.1: Advantages and limitations of Lead-acid batteries

Advantages	Inexpensive and simple to manufacture; low cost per watt-hour Low self-discharge; lowest among rechargeable batteries High specific power, capable of high discharge currents Good low and high-temperature performance
Limitations	Low specific energy; poor weight-to-energy ratio Slow charge; fully saturated charge takes 14-16 hours Must be stored in charged condition to prevent sulfation Limited cycle life; repeated deep-cycling reduces battery life The flooded version requires watering Transportation restrictions on the flooded type Not environmentally friendly

2.5 Lithium-ion battery

Lithium is the lightest of all metals, has the greatest electrochemical potential and provides the largest specific energy per weight. Rechargeable batteries with lithium metal on the anode could provide high energy density. The inherent instability of lithium ions caused unwanted dendrites (finger-like projections). These dendrites pass through the separator and cause an electrical short. Another drawback is that the cell temperature would rise quickly and approach the melting point of lithium causing thermal runaway.

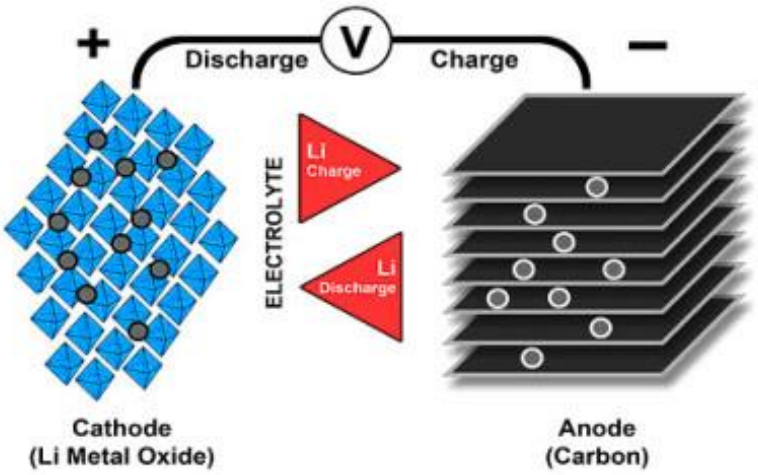

Figure 2.5: Ion flow in lithium-ion battery

The inherent stability of lithium metal especially during charging shifted the researchers to a non-metallic solution using lithium ions. In 1991, Sony commercialized the first Li-ion battery.

Lithium-ion is a low maintenance battery. It also has no memory and doesn't need exercising to keep it in good shape. Self-discharge is less than that of nickel-based systems. The main drawback is the cost of the lithium-ion battery and the need for protection circuits to prevent abuse.

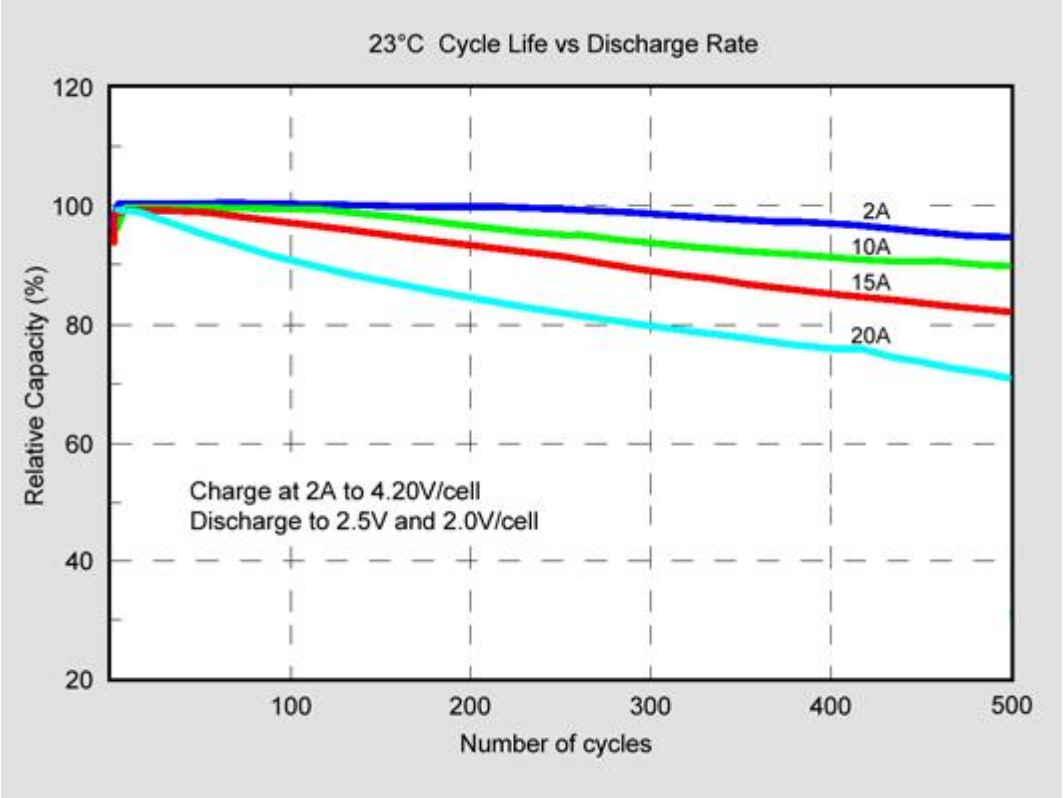

Figure 2.6: Cycle characteristics of Lithium-ion battery

Lithium-ion manufacturers specify the rise of internal resistance and self-discharge as a function of cycling, Advancements have been made with electrolyte which helps to keep the resistance low. The self-discharge of Li-ion is normally low but can be increased if misused.

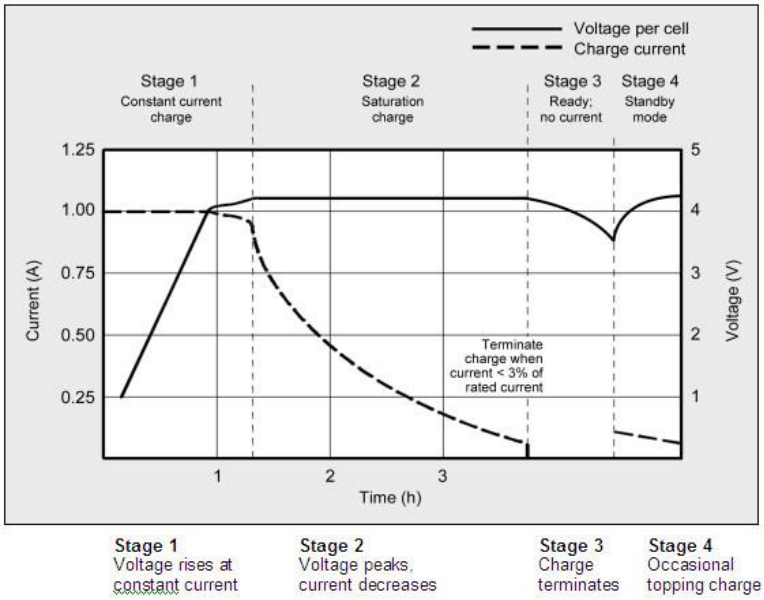

Figure 2.7: Charge stages of Lithium-ion

Charging and discharging of batteries is considered to be a chemical reaction, but in Li-ion it is claimed to be an exception. Scientists claim that the energy flow in this battery is a part of ion movement between anode and cathode. This is not completely true because if this was the case the battery should live forever. The reason given for this demerit is that the ions get trapped along with other reasons such as internal corrosion and other degenerative effects also known as parasitic reactions on the electrode and electrolyte. Old Li-ion batteries take a longer time to charge even if there is little to fill. A common ageing effect of Li-ion is loss of charge transfer capability. This is caused by the formation of passive materials on the electrodes, which inhibits the flow of free electrons. The ageing phenomenon is permanent and cannot be reversed.

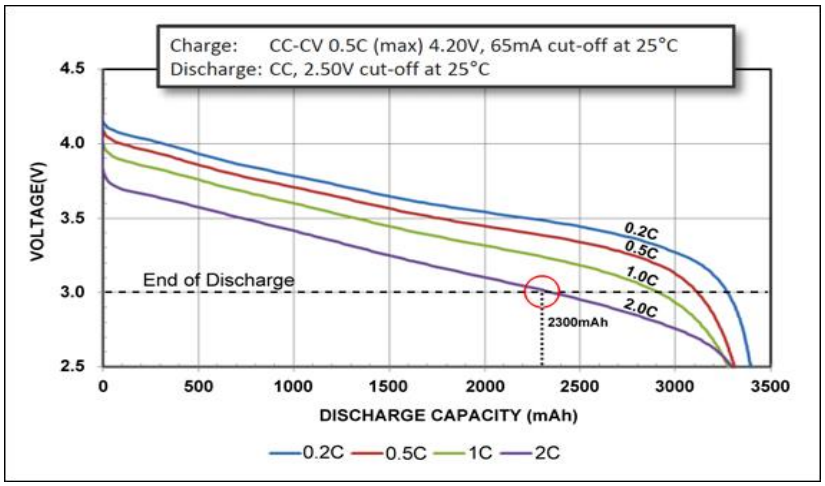

Figure 2.8: Discharge characteristics of NCR18650B Energy Cell

The Li-ion energy cell is made for maximum capacity to provide long runtimes. At the discharge cut off of 3.0V/cell, the discharge produces only 2.3Ah rather than the specified 3.2Ah. Therefore, this cell is used for light duties like portable computing. On the other hand, the Li-ion Power cell has a moderate capacity but excellent load capabilities. Therefore, this cell works for applications requiring heavy load current such as power tools.

Table 2.2: Advantages and Disadvantages of Li-ion battery

Advantages	High specific energy and high load capabilities with Power Cells
	Long cycle and extend shelf-life; maintenance-free
	High capacity, low internal resistance, good coulombic efficiency
	Simple charge algorithm and reasonably short charge times
	Low self-discharge (less than half that of NiCd and NiMH)
Limitations	Requires protection circuit to prevent thermal runaway if stressed
	Degrades at high temperature and when stored at high voltage
	No rapid charge possible at freezing temperatures (<0°C, <32°F)
	Transportation regulations required when shipping in larger quantities

2.6 Types of Lithium-ion battery

Li-ion batteries come in many varieties but all have one thing in common – the "lithium-ion" catchword. Although strikingly similar at first glance, these batteries vary in performance and the choice of active materials gives them unique personalities.

2.6.1 Lithium Cobalt Oxide (LCO)

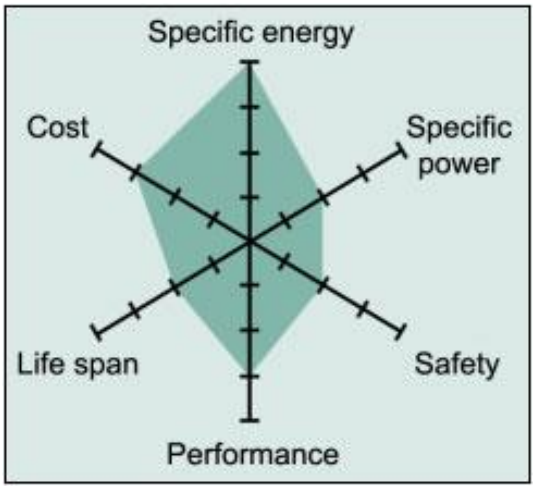

Figure 2.9: Snapshot of an average LCO battery

Li-cobalt battery consists of cobalt oxide cathode and a graphite carbon anode. The cathode has a layered structure and during discharge, Li ions move from anode to cathode. This flow reverses on charge. It has high specific energy which makes it a popular choice for digital cameras, mobile phones and laptops. The main drawbacks of Li-cobalt is a relatively short life span, limited load capabilities and low thermal stability.

2.6.2 Lithium Manganese Oxide (LMO)

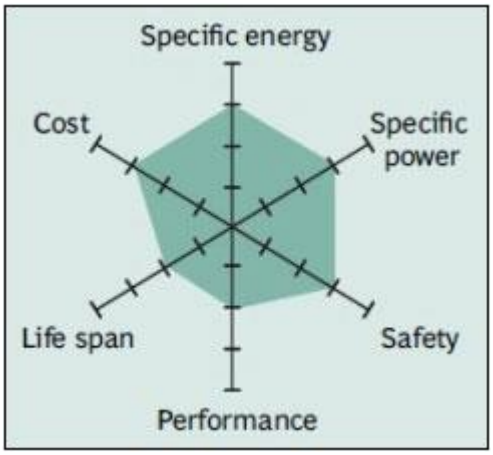

Figure 2.10: Snapshot of an average LMO battery

Manganese oxide is used as the cathode material. The architecture of LMO forms a three-dimensional spinel structure that improves ion flow on to the electrode, which results in lower internal resistance and improved current handling. It also has high thermal stability. The main drawbacks are limited calendar and cycle life.

2.6.3 Lithium Nickel Manganese Cobalt Oxide (NMC)

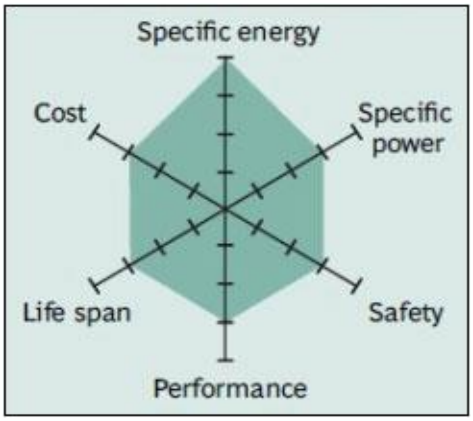

Figure 2.11: Snapshot of NMC

One of the most successful Li-ion systems is a cathode made up of nickel-manganese-cobalt (NMC). The secret of NMC lies in combining nickel and manganese. Nickel is known for its high specific energy but poor stability; manganese has the benefit of forming a spinel structure to achieve low internal resistance but offers low specific energy. Combining the metals enhances each other strengths. The cathode combination is typically one-third nickel, one-third manganese and one-third cobalt, also known as 1-1-1. A successful combination is NCM532 with 5 parts nickel, 3 parts cobalt and 2 parts manganese. Other combinations are NMC622 and NMC811. Silicon added to graphite has the drawback that the anode grows and shrinks with charge and discharge, making the cell mechanically unstable.

2.6.4 Lithium Iron Phosphate (LFP)

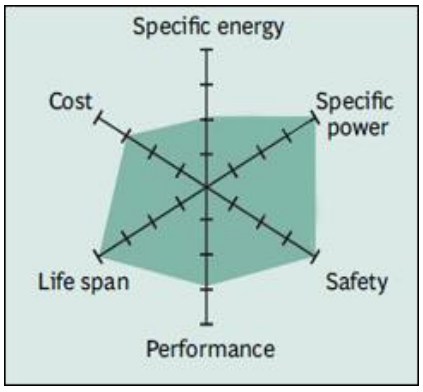

Figure 2.12: Snapshot of typical LFP battery

In this type of batteries, phosphate is used as cathode material. With nanoscale phosphate cathode material good electrochemical performance and low resistance are achieved. The key benefits are long cycle, tolerance to full charge conditions and have a long cycle life.

The main drawback is the reduction in nominal voltage (3.2V/cell) which eventually reduces the specific energy of the battery.

2.6.5 Lithium Nickel Cobalt Aluminum Oxide (NCA):

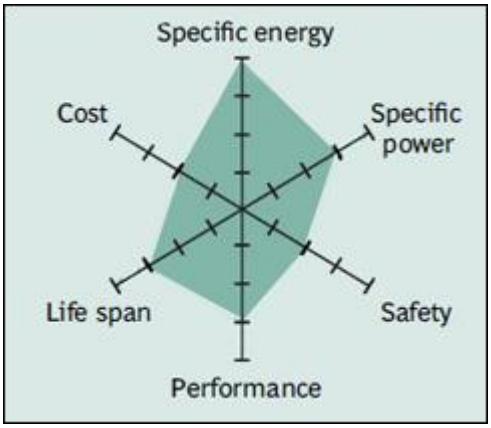

Figure 2.13: Snapshot of NCA

NCA is a further development of lithium nickel oxide; adding aluminum gives the chemistry greater stability. High energy and power densities, as well as a good life span, make NCA a candidate for EV powertrains. High cost and marginal safety are negatives.

2.6.6 Lithium Titanate (LTO)

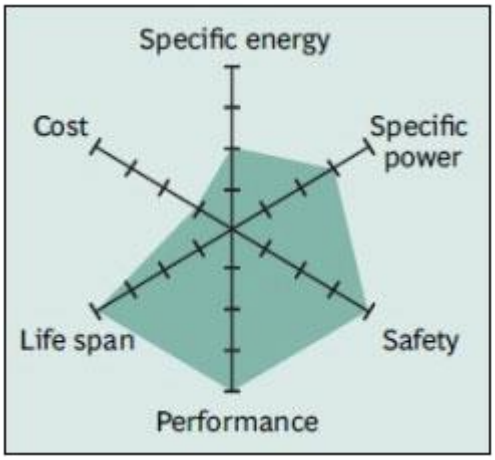

Figure 2.14: Snapshot of Li-titanate

Li-titanate replaces the graphite in the anode of a lithium-ion battery and the material forms into a spinal structure. The cathode can be lithium manganese oxide or NMC. Some advantages of this configuration are attaining zero strain property, thermal stability and the major drawback is that it is costly and has a low specific energy. Typical uses are electric powertrains, UPS and solar-powered street lighting.

2.7 Packaging of battery cells

Initially, the batteries are packed in glass jars but as size increased it shifted to wooden containers and then to composite materials. Some of the standard packaging of the batteries are given below:

Table 2.3: Different type of packaging of battery cells

Size	Dimensions	History
F cell	33 x 91 mm	Introduced in 1896 for lanterns; later used for radios; only available in nickel-cadmium today.
E cell	N/A	Introduced ca. 1905 to power box lanterns and hobby applications. Discontinued ca. 1980.
D cell	34.2 x 61.5mm	Introduced in 1898 for flashlights and radios; still current.
C cell	25.5 x 50mm	Introduced ca. 1900 to attain smaller form factor.
Sub-C	22.2 x 42.9mm 16.1mL	Cordless tool battery. Other sizes are ⅔, 4/5 and 5/4 sub-C lengths. Mostly NiCd.
B cell	20.1 x 56.8mm	Introduced in 1900 for portable lighting, including bicycle lights in Europe; discontinued in in North America in 2001.
A cell	17 x 50mm	Available in NiCd, NiMH and primary lithium; also in 2/3 and 4/5 sizes. Popular in older laptops and hobby applications.
AA cell	14.5 x 50mm	Introduced in 1907 as penlight battery for pocket lights and spy tool in WWI; added to ANSI standard in 1947.
AAA cell	10.5 x 44.5mm	Developed in 1954 to reduce size for Kodak and Polaroid cameras. Added to ANSI standard in 1959.
AAAA cell	8.3 x 42.5mm	Offshoot of 9V, since 1990s; used for laser pointers, LED penlights, computer styli, headphone amplifiers.
4.5V battery	67 x 62 x 22mm	Three cells form a flat pack; short terminal strip is positive, long strip is negative; common in Europe, Russia.
9V battery	48.5 x 26.5 x 17.5mm	Introduced in 1956 for transistor radios; contains six prismatic or AAAA cells. Added to ANSI standard in 1959.
18650	18 x 65mm 16.5mL	Developed in the mid-1990s for lithium-ion; commonly used in laptops, e-bikes, including Tesla EV cars.
26650	26 x 65mm 34.5mL	Larger Li-ion. Some measure 26x70mm sold as 26700. Common chemistry is $LiFeO_4$ for UPS, hobby, automotive.
14500	14x 50mm	Li-ion, similar size to AA. (Observe voltage incompatibility: NiCd/NiMH = 1.2V, alkaline = 1.5V, Li-ion = 3.6V)
21700*	21 x 70mm	New (2016), used for the Tesla Model 3 and other applications, made by Panasonic, Samsung, Molicel, etc.
32650	32 x 65mm	Primarily in $LiFePO_4$ (Lithium Iron Phosphate)

Under this different packaging types are used for different purposes. The cylindrical cells are used in flashlights, TV remotes etc. and the planar rectangular type of batteries are commonly seen in mobile phones and laptops. These varieties arise to increase the portability of devices.

2.8 Series and parallel configuration of battery

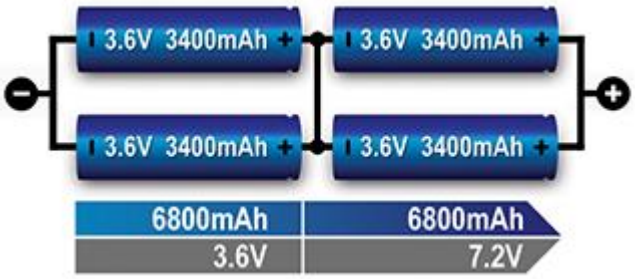

Figure 2.15: Representation of series and parallel combination

A single cell doesn't cater to all of our needs and therefore we need to combine them to attain our objective. The series connection increases the voltage rating whereas the parallel combination increases the current rating. The battery industry specifies the number of cells in series first, followed by the cells placed in parallel. An example is 2s2p.

CHAPTER III

STATE OF CHARGE

3.1. Introduction:

- State of Charge (SoC) is the level of charge of an electrical battery relative to its rated capacity. The units of SoC are represented in percentages.
  For Ex: - 0% = empty; 100% = full
- Another way to measure the same is the Depth of Discharge (DoD). It is the inverse of SoC.
  For Ex: - 100% = empty; 0% = full.
- SoC is normally used when discussing the current state of a battery in use, while DoD is discussed about the lifetime of the battery after repeated use.
- In a battery electric vehicle (BEV), the SoC of the battery is analogous to the fuel gauge of an IC engine.
- Even in PHEV, the reserved hybrid work is used when the motors are needed to be accelerated. The engine acts as a generator and charges the batteries so that it can give the desired output.

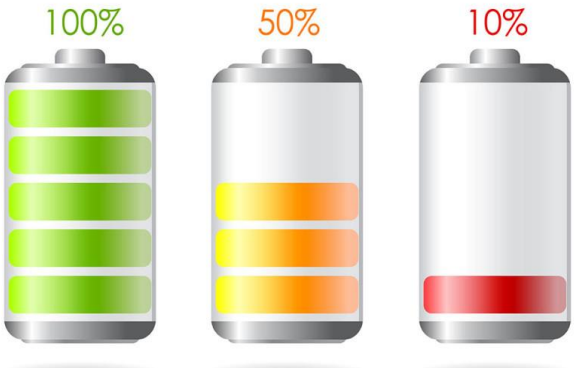

Figure 3.1: State of charge

3.2 Current techniques to determine SoC

Usually, SoC cannot be obtained or measured directly instead it is estimated from direct measurement variables. This estimation is carried out through the following processes-

3.2.1 Chemical method

This method works only with those types of batteries that offer access to their liquid electrolyte. The specific gravity or pH of the electrolyte can be used to estimate the SoC of a battery. Hydrometers are used to calculate the specific gravity of the battery. In recent times the refractometry methods are being used because the refractive index of the battery is directly proportional to the specific gravity of the electrolyte.

3.2.2 Voltage method

In this method, the voltage of the battery is initially concerned. From this reading, SoC is derived using the known discharge curve (Voltage vs. SoC) of the battery. The voltage of a battery is affected by battery and temperature. Therefore, this method's accuracy can be increased by a correction term proportional to battery current and by using a table of the battery's open-circuit voltage vs temperature.

But in reality, we try to keep voltage constant regardless of SoC, which makes this method difficult to apply.

3.2.3 Current integration method

This method is also known as the coulomb counting method. In this method, the discharging current of a battery is monitored. This discharging current is integrated over time in order to estimate SoC. Let the current or the value of SoC to be estimated is SoC(t), I(t) is the discharging current and SoC(t-1) be the previously estimated SoC then the SoC is estimated based on the following equation:

$$SoC(t) = SoC(t\text{-}1) + I(t)ndt.$$

The drawback of this method is that it doesn't consider the effects of temperature, battery history, discharge current and cycle life.

3.2.4 Kalman Filter

To overcome the disadvantages of the Voltage method and current integration method, a Kalman filter is used. The battery can be modelled electrically in such a way that we can use the Kalman filter to predict the overvoltage due to current. The application of the Kalman filter is to provide SoC estimations for the battery via real-time state estimation. An EKF is used to estimate the concentrations of the main chemical species which are

averaged on the thickness of the active material to obtain the SoC of the battery. For a battery, the UKF method of SoC estimation is superior to that of the EKF method of SoC estimation.

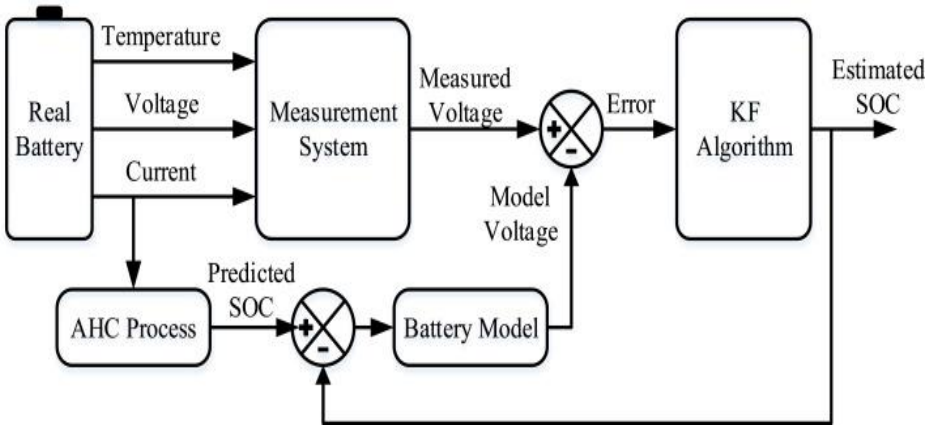

Figure 3.2: SoC estimation using Kalman Filter

3.2.5 Combined approaches

The main theme of the combined approaches is to bring about the advantages of each filter and obtain an optimized solution. There are three types of combined or hybrid models:

3.2.5.1 Coulomb counting and EMF combination

This method combines the direct measurement method with the battery EMF measurement during the equilibrium state. Any battery will lose capacity during cycling. In order to calculate SoC and remaining run time (RRT) accurately and also to consider the ageing effect, a simple Qmax algorithm is proposed. This method can also be applied to a new battery. Since a battery loses capacity as its age passes the accuracy of predicting SoC and RRT increases.

3.2.5.2 Coulomb counting and KF combination

This method is generally denoted as the “KalmanAh method”. It uses the Kalman filter method to make the approximate initial value converge to the real value. Then the coulomb counting method is used to estimate the SoC for a long working time. The error obtained in this method is 2.5% of the real SoC when compared to 11.4% when using the Coulomb counting method.

3.2.5.3 Per unit system and EFK combination

Extended Kalman Filter (EFK) combined with a per-unit (PU) system is used to identify the suitable battery model parameters to estimate SoC more accurately of a lithium-ion degraded battery. All the parameters considered including terminal voltage and current are converted into dimensionless values relative to a base value. These converted values are applied to dynamic and measurement models in the EKF algorithm.

3.2.6 Advanced methods

SoC estimation is a very challenging task as it is a nonlinear function of temperature and current Data-driven techniques for SoC estimation have comparatively higher prediction accuracy when compared to traditional methods. as they are based on data science and machine learning algorithms. With advancements in Artificial Intelligence (AI), machine learning is being used extensively in different domains like infotainment, driver assistance systems, autonomous vehicles etc. This encourages and suggests to us that AI techniques can be used in determining an efficient prediction strategy that is best suited, accurate, adaptive and is capable of estimating SoC precisely.

AI techniques for regression are categorized as, linear regression, decision trees, Support Vector Machine (SVM) and neural networks. The former two techniques are efficient for linear data. Battery exhibits nonlinear characteristics; hence the work focuses on using Artificial Neural Networks (ANN) and SVM models for accurate SoC estimation. There are also other techniques like Long short-term memory (LSTM) and Convolution neural networks (CNN).

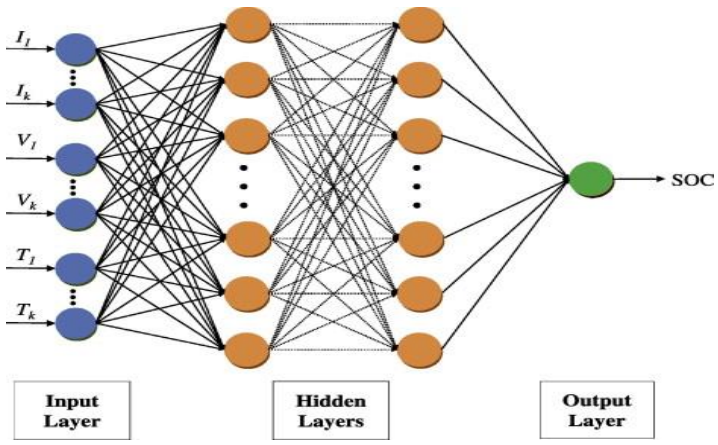

Figure 3.3: SoC estimation using ANN

CHAPTER IV

SoC Prediction

4.1 Prediction of SoC

SoC indicates the residual charge inside a battery cell and is indicated in the form of percentage. Hence one can identify the charge of a battery by checking its SoC value. SoC Prediction therefore predicts how much charge will be left in a battery after its usage.

$$SOC(t) = Q(t)/Q_n$$

The traditional methods used to SoC are as follows

4.2 Direct Measurements [1]

Direct Measurements refers to some physical battery properties such as terminal voltage and impedance. Various Direct Measurements include

4.2.1 Open Circuit Voltage

Approximately a linear relationship between the SOC of battery and its open circuit voltage (OCV) given by:

$$V_{OC}(t) = a_1 \times SOC(t) + a_0$$

Where SOC(t): SOC of battery at time t

a_0 : Battery terminal voltage when SOC = 0%

a_1 : Coefficient obtained by knowing at a_0 SOC=100%

The OCV method is proportional to the SOC when they are disconnected from the loads for a period longer than two hours. The OCV relationship with SOC was decided by applying a pulse load on the Li-ion battery, then allowing the battery to attain equilibrium. Because the traditional OCV-SOC differs among batteries, there's a drag therein the connection of the OCV-SOC should be measured to estimate accurately the SOC. The SOC and the capacity of a lithium-ion battery are estimated using the dual extended Kalman filter with the proposed method.

The graph shows the SOC percentage v/s OCV of a Lithium-Ion battery. As shown in graph the OCV (V) increases with SOC and hence they are directly proportional to each other.

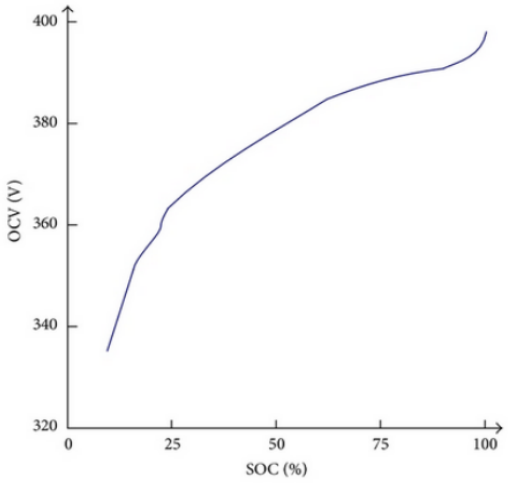

Figure 4.1: SOC (%) v/s OCV (V) for Li-Ion battery

4.2.2 Kalman Filter

Kalman filters help in estimating the variables of interest when they can't be measured directly, but an indirect measurement is out there. They are also useful for finding the best estimate of states by combining measurements from various sensors in the presence of noise.

Using real-time data to estimate the SOC of a battery would normally be difficult or expensive to measure. Hence, we use a Kalman filter to provide verifiable estimations of SOC for the battery via the real-time state estimation.

4.2.3 Coulomb Counting Method

The Coulomb counting method measures the discharging current of a battery and integrates the discharging current over time in order to estimate SOC [20]. Coulomb counting method is done to estimate the, which is estimated from the discharging current, and previously estimated SOC values, SOC is calculated by the following equation:

$$SOC(t) = SOC(t-1) + (I(t)/Q_n)\Delta t$$

Other factors that affect Coulomb Counting Method includes

1. Temperature
2. Battery History

3. Discharge Current
4. Cycle Life

Modern Methods to predict SOC includes using various Machine Learning Algorithms and modelling them for the same. Here are some of the Algorithms that can be used for the same:

4.3 ML Algorithms

4.3.1 Support Vector Machine (SVM)

SVM is used for classification as well as regression problems. The main goal of SVM is to create the best line or decision boundary. This decision boundary is called a hyperplane. SVM chooses the extreme points/vectors that help in creation of hyperplane. These extreme cases are called support vectors and hence the algorithm is called the Support Vector Machine.

Types of SVM

1. 1 Linear SVM

Linear SVM is used against linearly separable data which means that if a dataset can be classified into two classes by using a single straight line, then such data is termed linearly separable data, and classifier is used as Linear SVM classifier.

The following figure shows a linear SVM where data can be classified linearly along with the plane of separation.

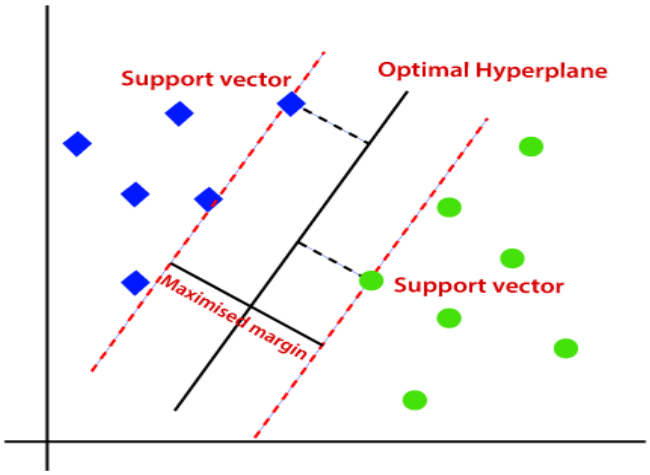

Figure 4.2: Linear SVM

Working

The working of the SVM algorithm can be understood by using an example. Suppose we have a dataset that has two tags (green and blue), and the dataset has two features x1 and x2. We want a classifier that can classify the pair (x1, x2) of coordinates in either green or blue. So as it is 2-d space so by just using a straight line, we can easily separate these two classes. But there can be multiple lines that can separate these classes.

1.2 Non-Linear SVM

Non-Linear SVM is used for non-linear data sets. If data is linearly arranged, then we can separate it by using a straight line, but for non-linear data, we cannot draw a single straight line. So to separate these data points, we need to add one more dimension. For linear data, we have used two dimensions x and y, so for non-linear data, we will add a third dimension z. It can be calculated as: $z = x^2 + y^2$. Since we are in 3-d Space, hence it is looking like a plane parallel to the x-axis. If we convert it in 2d space with z=1.

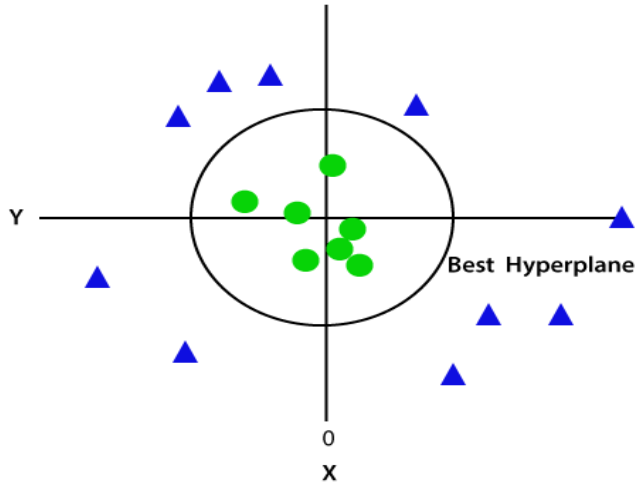

Figure 4.3: Non-Linear SVM

Applications of SVM:

- SoC Estimation
- Fault Detection
- Face Detection
- Classification of images

4.3.2 Artificial Neural Network (ANN)

Artificial Neural Network (ANN) is called neural networks are computer systems vaguely inspired by the biological neural networks that constitute animal brains. An ANN is based on a collection of connected units or nodes called artificial neurons which loosely model the neurons in a biological brain. An artificial neuron receives a signal then processes it and then signals the other neurons connected to it.

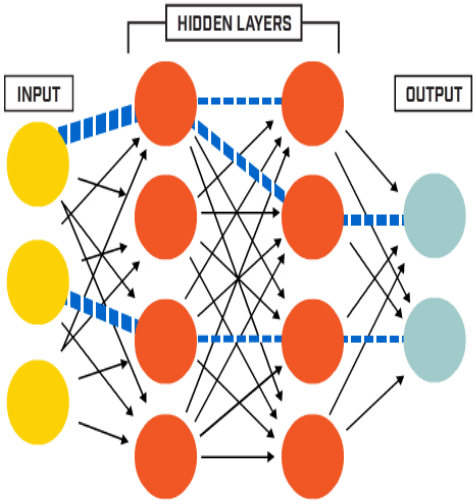

Figure 4.4: ANN Structure

The ANNs have the ability to work under a nonlinear environment and most of the daily life situations we deal with are nonlinear or non-uniform. The results obtained by using this method have high accuracy. ANN method does not require extensive domain knowledge and also has shorter development time along with good accuracy and less cost. Neural Networks have the ability to learn by themselves and produce the output that is not limited to the input provided to them.

Network Layers of ANN:

- Input Layer
- Hidden Layer
- Output Layer

The input different layers are connected by synapses also known as edges. The edges have a weight which gets adjusted during the training. The ANNs use the Back Propagation

Neural Network (BPNN) algorithm for training. The BPNN aims to calculate the desired output value by updating the weight in the network at every epoch. The difference between the output of the neural network and the desired target is nothing but the cost function.

Working

- Initially the weighted sum of n input variables is calculated.
- The weighted cost is calculated as the sum of product of individual inputs with their corresponding weights.
- The activation function activates the output based on the parameters.
- The most predominant activation functions are Threshold function, Sigmoid function, Hyperbolic tan function and Rectifier function.
- During training the weights of the edges are adjusted with the help of BPNN algorithm using the cost function.

Mathematical Representation

$$O_j = f_j \Sigma (w_{jk} x_k)$$

Where O_j = Output of neuron

F_j = Transfer Function

W_{jk} = Adjustable weight that shows strength of each neuron

X_k = Input to neuron

Applications:

- State of Charge estimation of Li ion battery
- Electrical price optimisation
- Short term load forecasting
- Fault analysis

4.3.3 Long Short-Term Memory (LSTM)

Long Short-Term Memory (LSTM) is a variety of recurrent neural networks (RNNs) that are capable of learning long-term dependencies. LSTM has feedback connections, i.e., it is capable of processing the entire sequence of data, apart from single data points such as images. This is a behavior required in complex problem domains like machine translation,

speech recognition, and more. They are networks with loops in them, allowing information to persist.

Unlike RNNs, LSTM is free from Long Dependencies Problems. Traditional neural networks can't do this, and it seems like a major shortcoming. Instead of having a single neural network layer, there are four, interacting in a very special way.

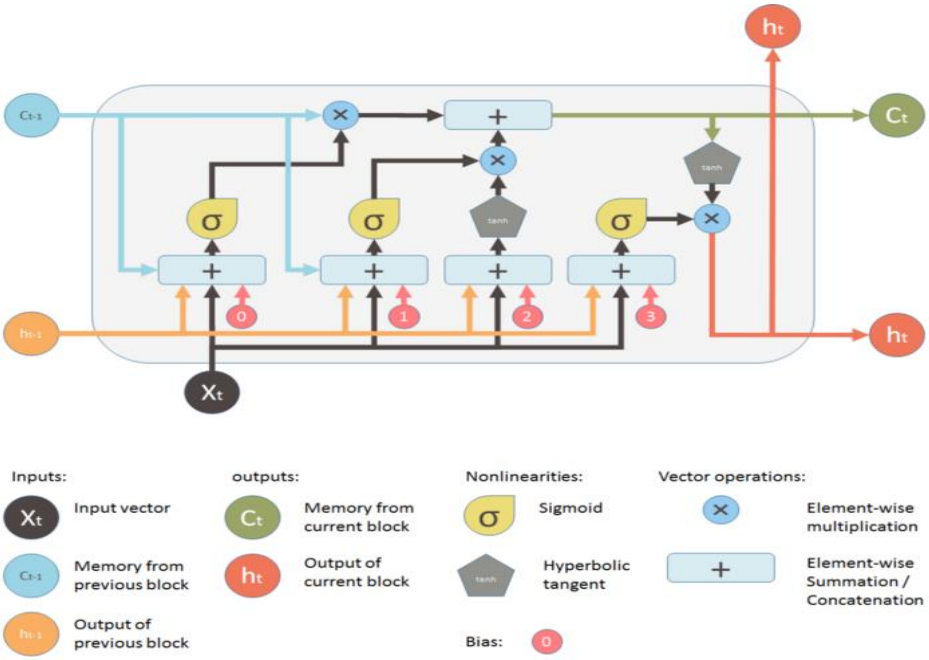

Figure 4.5: LSTM Algorithm Structure

Working

- The first step in LSTM is to decide what information to throw away from the cell state. This decision is made by a sigmoid layer called the "forget gate layer."

$$F_t = \sigma(W_f \,.\, [h_{t-1}, x_t] + b_f)$$

- The next step is to decide what new information we're going to store in the cell state. This has two parts.
  - First, a sigmoid layer called the "input gate layer" decides which values we'll update.
  - Next, a tanh layer creates a vector of new candidate values, C_t, that could be added to the state

$$I_t = \sigma(W_i \,.\, [h_{t-1}\,,\, x_t\,] + b_i)$$

$$C_t = \tanh(W_C \,.\, [\,h_{t-1}\,,\, x_t\,] + b_C)$$

- Update the old cell state, C_{t-1}, into the new cell state C_t.
- We multiply the old state by f_t (0-1). Then we add $i_t * C_t$. This is the new candidate value, scaled by how much we decided to update each state value

$$C_t = f_t * C_{t-1} + i_t * \tilde{C}_t$$

- And finally, we need to generate the output for this LSTM unit. This step has an output valve that is controlled by the new memory, the previous output h_{t-1}, the input X_t and a bias vector. This valve controls how much new memory should be output to the next LSTM unit.

$$O_t = \sigma(W_o . [h_{t-1}, x_t] + b_o)$$

$$H_t = o_t * \tanh(C_t)$$

Applications of LSTM

- ❖ SoC Estimation
- ❖ Short Term Forecasting for Renewable Energy
- ❖ Fault Prediction
- ❖ Energy Demand Forecasting
- ❖ Fault Diagnosis of Induction Motor

4.3.4 Random Forest

The random forest is a classification/supervised learning algorithm consisting of many decision trees and builds multiple decision trees and merges them together to get a more accurate and stable prediction. It uses bagging and features randomness to build each individual tree to create an uncorrelated forest of trees. Advantages of random forest include that it can be used for both classification and regression problems.

We need features that have at least some predictive powers. The trees of the forest and their predictions need to be uncorrelated. The features we select and the hyper-parameters we choose will impact the ultimate correlations.

Feature Randomness

In a normal decision tree, when it is time to split a node, we consider every possible feature and pick the one that produces the most separation between the observations. In contrast,

each tree in a random forest can pick only from a random subset of features. This forces even more variation amongst the trees in the model and ultimately results in lower correlation across trees and more diversification.

Bagging

With bagging we are not sub setting the training data into smaller chunks and training each tree on a different chunk. Rather, we take a random sample of size N with replacement. For example, if our training data was [1, 2, 3, 4, 5, 6] and N=6 then we might give one of our trees the following list [1, 2, 2, 3, 6, 6]. This enhances the decision-making process.

Working

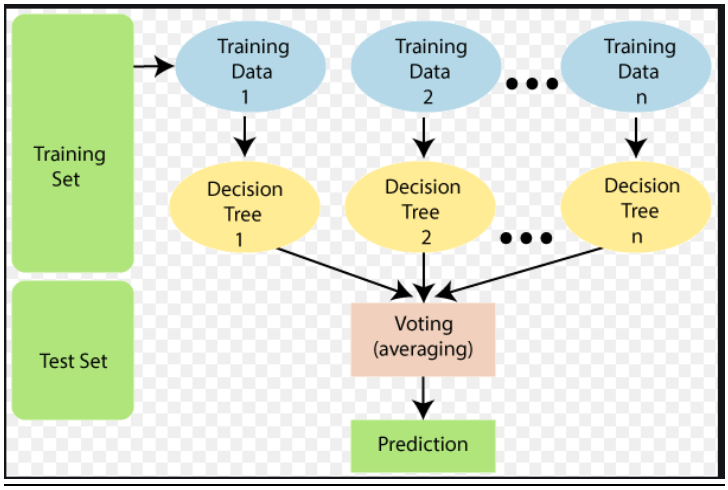

Figure 4.6: RF Structure

Decision trees involve the greedy selection of the best split point from the dataset at each step. Example formula for decision tree is:

$$Ni_j = w_jC_j - W_{left(j)}C_{left(j)} - W_{right(j)}C_{right(j)}$$

Where,

Ni_j = Importance of node j

w(j) = Weighted number of samples reaching node j

C(j) = Impurity of node j

Applications:

- Short Term Forecasting
- Electricity price Forecasting
- Electricity Theft Detection

CHAPTER V

SoC Estimation modelling and its performance

In this work, experimentation with various networks is performed, both traditional and advanced algorithms [5]. We initially modelled feed-forward neural networks on NASA dataset then synthesized data using simulator. This synthesized data was trained on both traditional as well as advanced algorithms. For traditional we used Extended Kalman Filter. Finally, a combined CNN-LSTM network is developed to model the highly non-linear dynamics of lithium-ion batteries and estimate SoC from measurable voltage, current and temperature variables.

5.1 Data Generation

In this phase sensory data is collected according to input variables definition, in order to build a raw dataset for the experiment. Main input variables are: measurable voltage, current, temperature and current SoC. This phase is mainly defined to collect and transfer data for pre-processing.

5.1.1 NASA Dataset

An analysis of battery No.06, No.07, and No.18 degradation datasets obtained from NASA Ames Prognostics Center of Excellence (PCoE) database [6] was conducted to validate the effectiveness of the developed FNN approach. The dataset of battery No.05 was used as a training dataset for all algorithms.

This dataset contains the test results of the experiment that has been performed under controlled conditions in the NASA testbed of commercially available lithium-ion 18650-sized rechargeable batteries.

Data were obtained from 3 different lithium-ion battery operation test conditions: charge, discharge, and impedance. Until the voltage reached 4.2 V, charge was performed at a constant current of 1.5 A and then until the charge current dropped to 20 μA, the battery continued charging at a constant voltage. The

discharge was also performed at a constant current of 2 A until the voltage dropped to 2.7 V, 2.5 V, 2.2 V, and 2.5 V. Electrochemical Impedance Spectroscopy frequency adjustment from 0.1 kHz to 5 kHz was used to do the impedance test. The aging characteristics of the batteries was accelerated by repeatedly performing charge and discharge tests in multiple cycles. The tests were stopped when the batteries reached the end-of-life criteria, which was defined as a 30% fade from the rated capacity.

Based on the schematic diagram of the tested battery, below is the characteristic profile of the battery, which will be used as a training data set. Figure 5.2 shows some details of the current and voltage behaviors during the charging and discharging cycles of the battery.

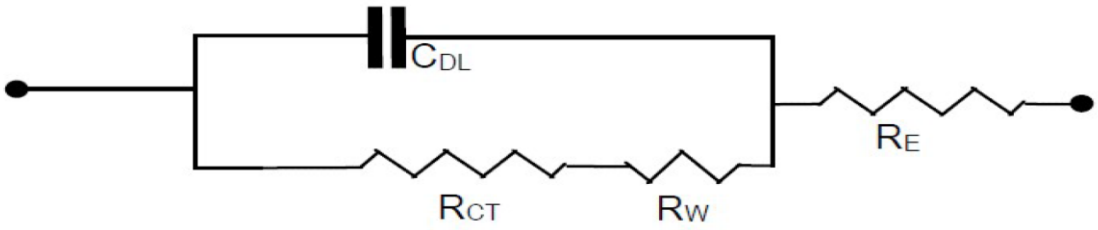

Figure 5.1 The schematic diagram of the tested battery.

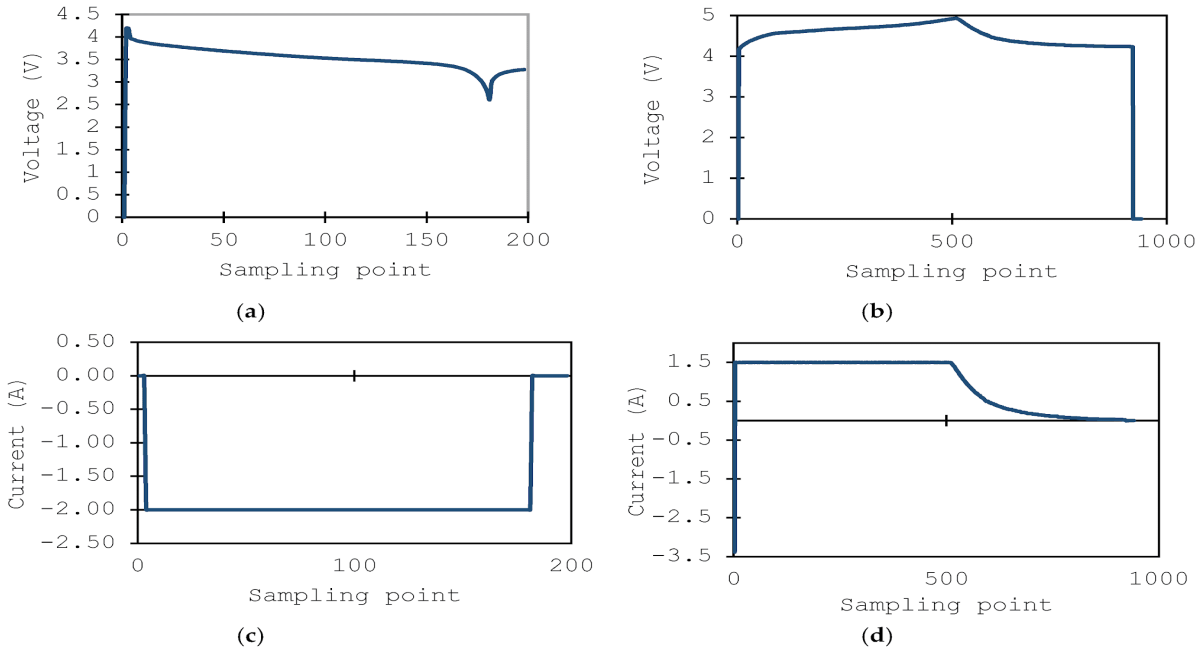

Figure 5.2 The current and voltage during the discharging and charging of battery No. 05: (a) the current of discharging, (b) the current of charging, (c) the voltage of discharging, and (d) the voltage of charging.

5.1.2 Synthesized Dataset

In the process of training the model, a large amount of data that can reflect the current state of the lithium battery is required. Data generation through physical experiments, many factors such as the high cost, high risk and experimental conditions of laboratory research needs to be taken care of. We use a simulator to generate data as this method of obtaining data from the environment will be more economical and efficient.

For battery modules, first, we use a more accurate PNGV equivalent circuit model to describe the current-voltage relationship of the actual lithium-ion battery. Secondly, we get the variation curve of the characteristics of each component with temperature and the capacity and level of the lithium-ion battery. A series of actual data such as terminal voltage, current SoC, open circuit voltage, current and real-time temperature of the previous state is measured and finally we calculate the current based on the power consumption, heating power and the initial state. In addition, we also considered the possible faults of the motor and battery, and for different faults performed analysis and early warnings.

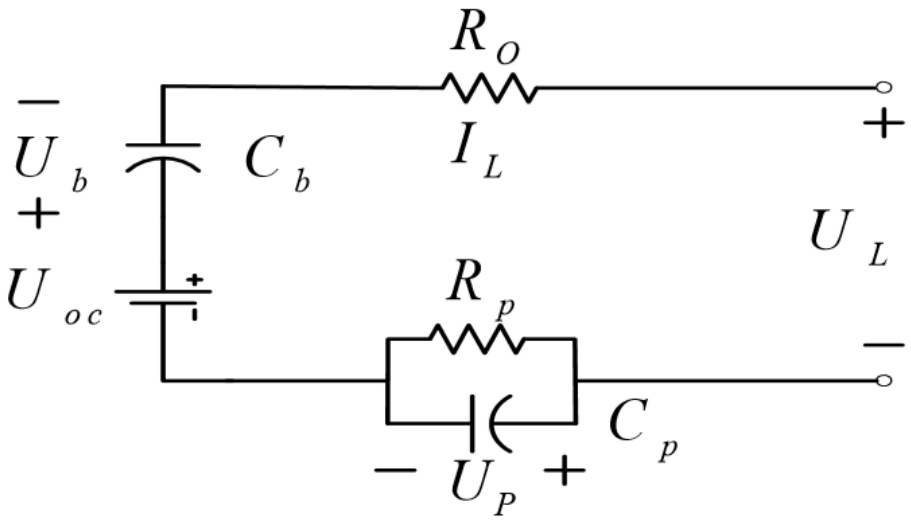

Figure 5.3 Equivalent circuit of PNGV Battery model

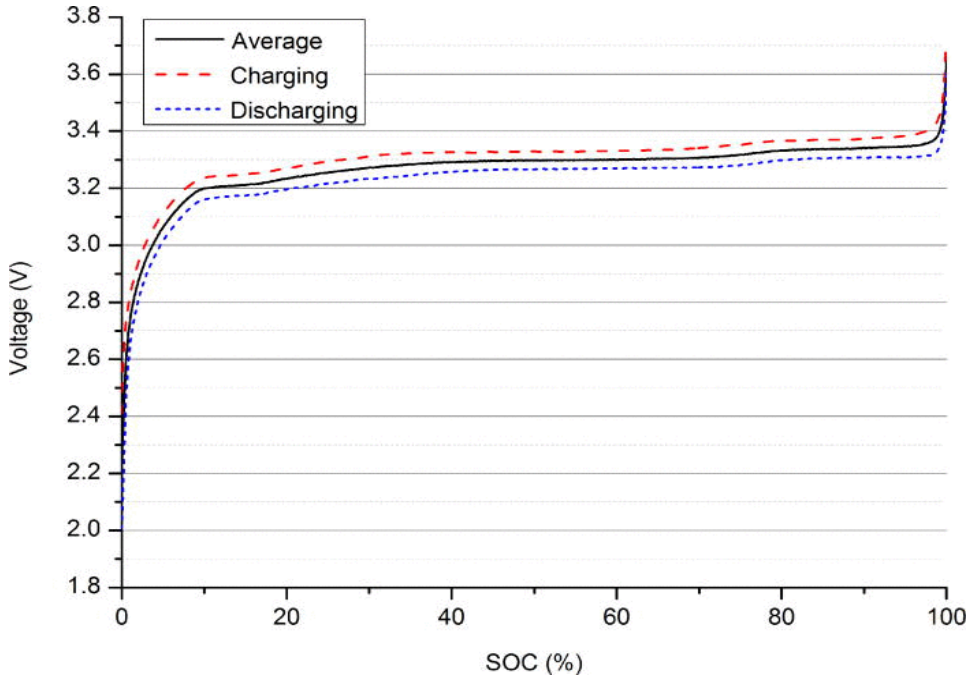

Figure 5.4 OCV-SoC characteristic of battery

5.2 Data Pre-processing

In this phase, collected sensory data according to the predefined input variables, in order to build a raw dataset for the experiment. The raw datasets are preprocessed and normalized, and then divided into a training and a testing dataset. [7]

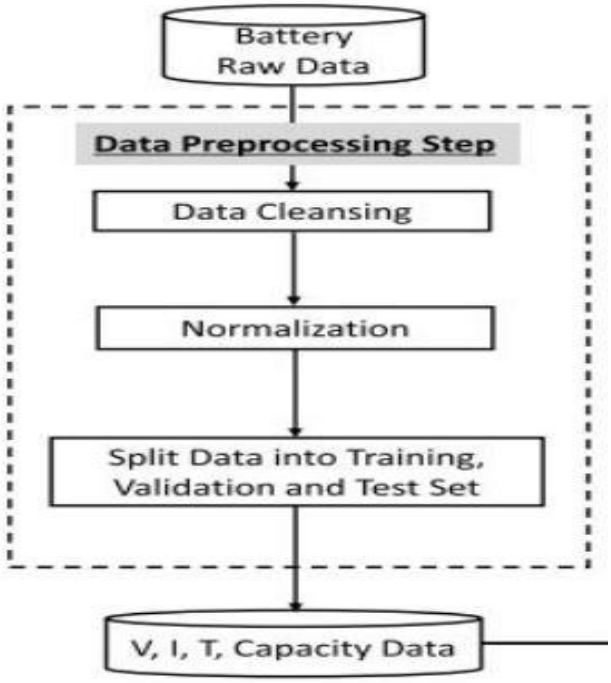

Figure 5.5 Data Pre-processing Framework

5.2.1 Data Cleansing

In this process, we detect and fix corrupt or inaccurate records from a record set, table, or database and identify incomplete, incorrect, inaccurate or irrelevant parts of the data and then replace, modify, or delete the dirty or coarse data.

We use python along with pandas library to remove unwanted observations from the dataset, including duplicate observations or irrelevant observations.

```
df = df.drop_duplicates()
```

and, drop observations that have missing values.

```
df = df.dropna()
```

5.2.2 Normalization

Data normalization is the organization of data to appear similar across all records and fields. It increases the cohesion of entry types leading to cleansing, lead generation, segmentation, and higher quality data.

This process includes eliminating unstructured data and redundancy in order to ensure logical data storage.

We use, min-max normalization for better training since it retains the original distribution of data except for a scaling factor and transforms all the data into the range of [0,1] as below:

$$z_i^k = \frac{x_i^k - min(x)}{max(x) - min(x)}$$

5.2.3 Data Splitting

In this process of partitioning data into two or three portions, usually for training and validation purposes. One portion of the data is used to develop and train the model and the other two to optimize and evaluate the model's performance.

In the training set, the data is used to fit the model, that is the first portion of the dataset that we use to train the model. The model observes and learns from this data and optimizes its parameters.

In the cross-validation set, we minimize the error in the trained model and reduce underfitting or overfitting of the trained model.

In the testing set, an impartial evaluation of the final model. It is used after the model is completely trained using the training and validation set. Therefore, the test set

replicates the type of situation that will be encountered by the model when deployed for real-time use.

5.3 Model Structure

In this phase, initial parameters are developed, and the model is trained by the training dataset, based on both traditional as well as advanced estimation theories. It is particularly important to fine-tune the classification model through misclassification errors such as RSME, MAE.

We analyzed the feed forward neural network, Kalman filter [8] and combined CNN-LSTM network.

5.3.1 Extended Kalman Filters

For linear dynamic systems to obtain unbiased, best estimation of state variables, standard Kalman filter (KF) is suitable. Equation of linear discrete system are as follows:

$$x_k = A_k x_k + B_k u_k + w_k$$
$$y_k = H_k x_k + D_k u_k + v_k$$

where x represents the n-dimensional system state vector; y represents the m-dimensional output vector of observations; u represents the one-dimensional input vector; A represents nxn system matrix; B is nxl input matrix; H is mxn output matrix; D is mxl feedforward matrix; w and v are all Gaussian white noise.

But power batteries are a non-linear dynamic system, while KF only applies to estimate the linear system. Therefore, non-linear systems need to be changed by linearization, which is approximately as a linear system, so the KF could be used to estimate the system state. This is called the extended Kalman filter (EKF). [9] Equation of nonlinear discrete system is as follows:

$$\begin{cases} x_{k+1} = f(x_k, u_k) + w_k \\ y_k = h(x_k, u_k) + v_k \end{cases}$$

where f represents the state transfer function of the nonlinear system; h represents the measuring function of nonlinear systems.

Nonlinear system linearization needs to be changed. Using Taylor series, the state transfer function and measurement function are defined, second and higher order terms are omitted. Results obtained after linearization are as follows:

$$\begin{cases} x_{k+1} \approx \hat{A}_k x_k + f(\hat{x}_k, u_k) - \hat{A}_k \hat{x}_k + w_k \\ y_k \approx \hat{C}_k x_k + h(\hat{x}_k, u_k) - \hat{H}_k \hat{x}_k + v_k \end{cases}$$

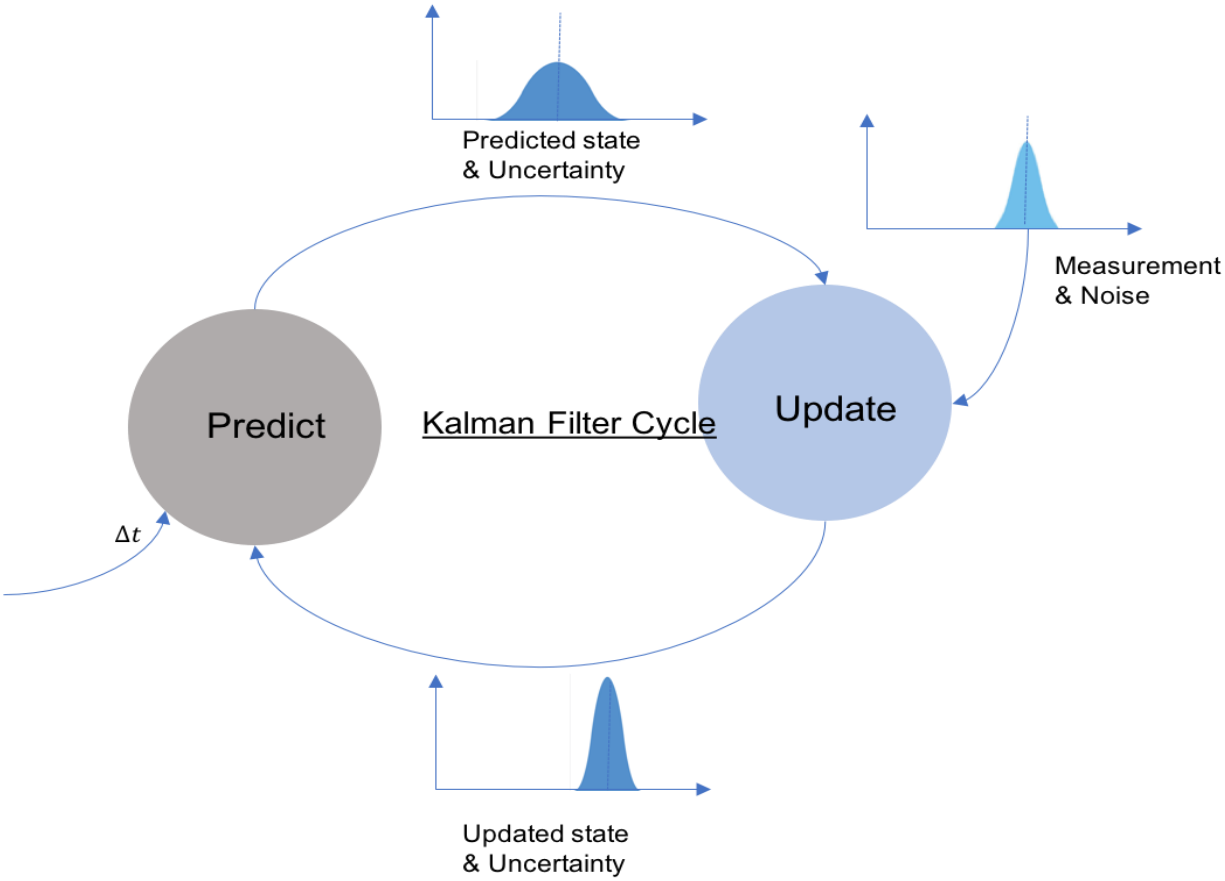

Figure 5.6 Kalman Cycle

Using synthesized dataset, the remaining battery charge SOC and the voltage across the RC circuit represent the system state variables, current represents input variable, and the battery terminal voltage represents output variable. [9] The final state equation and observation equation are as follow:

$$\begin{cases} \begin{bmatrix} s(k) \\ U_c(k) \end{bmatrix} = \begin{bmatrix} 1 & 0 \\ 0 & \exp(-T_s / C_p R_p) \end{bmatrix} \begin{bmatrix} s(k-1) \\ U_c(k-1) \end{bmatrix} \\ \qquad + \begin{bmatrix} T_s / Q_n \\ R_p (1 - \exp(-T_s / C_p R_p)) \end{bmatrix} [I(k-1)] + \begin{bmatrix} w_1(k-1) \\ w_2(k-1) \end{bmatrix} \\ U_t(k) = \begin{bmatrix} \frac{\partial U_{ocv}(s)}{\partial s} & -1 \end{bmatrix} \begin{bmatrix} s(k-1) \\ U_c(k-1) \end{bmatrix} + [-R][I(k-1)] + [v(k)] \end{cases}$$

where T, represents the sampling time, Q represents the rated capacity of the battery.

5.3.2 Deep Neural Network

Currently, deep neural networks (DNN) because of its promising performance and advantages have become a well-employed approach in machine learning. DNN employs a multi-layered feed-forward neural network [11], similar to the artificial neural network, but with fully-connected hidden layers.

The experiment was constructed by varying the number of dense layers in DNN, [12] the hidden layer was varied to analyze the SoC of battery data. To prevent the overfitting problem, the dropout layer [13] was also applied as the last layer before the output layer which randomly drops neurons during the model training, as shown in Figure 5.7. The neural network after being sampled, the so-called "thinned" network, will contain only the surviving neurons.

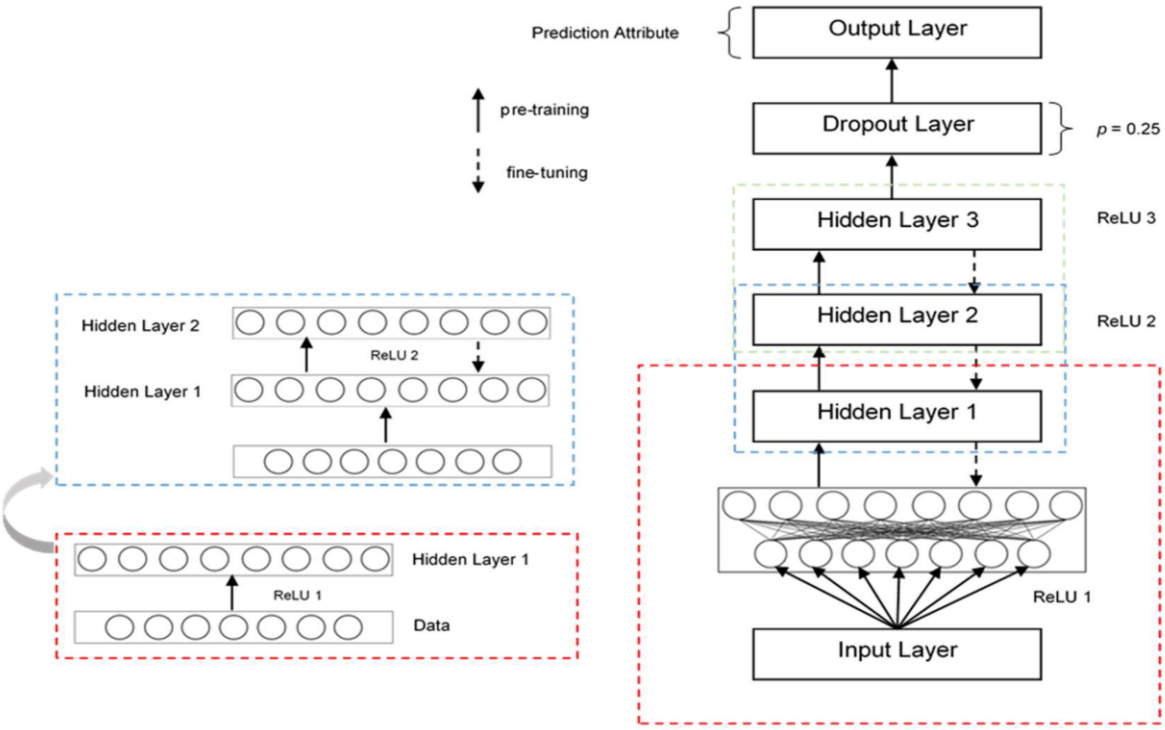

Figure 5.7 The deep neural network model.

Varying the hidden layers of DNN from 2 layers to 4 layers, the RMSE results from Table 5.1 show that the best formation of DNN consists of three fully-connected hidden layers, along with the ReLU activation function.

During the training process, mean square error (MSE) is chosen as the overall loss function which is evaluated at the end of each forward pass until we reach a global minima:

$$MSE = \frac{1}{K}\sum_{k=1}^{K}(y_k - \hat{y_k})^2$$

where y_k is the true SOC value while $\hat{y}_k$ is the output of the proposed network at time k.

Adam optimizer [14] is selected to minimize the total loss, which based on the gradient of the loss function updates the network weights and biases. The initial learning rate (alpha) is set to 0.01. The decay rates are set to 0.9 and 0.999, respectively. In the training phase, a dropout rate of 20% is used in the LSTM layer and fully connected layer.

The root means square error (RMSE) and mean absolute error (MAE) are used to evaluate the performance of the proposed network in the testing process:

$$\mathrm{RMSE} = \sqrt{\frac{1}{K}\sum_{k=1}^{K}(y_k - \hat{y}_k)^2}$$

$$\mathrm{MAE} = \frac{1}{K}\sum_{k=1}^{K}|y_k - \hat{y}_k|,$$

MAE measures how close the estimation is to the true values neglecting the sign whereas the RMSE characterizes the variation of errors and is more sensitive to large errors.

Table 5.1 RMSE results of each stacked hidden layer model.

Number of Hidden Layers	RMSE
2	3.815
3	3.247
4	3.275

5.3.3 CNN-LSTM Network

SoC has two kinds of features: first, the spatial feature which is the interrelations within current input and the temporal feature which is the correlations between current SOC and past inputs. A combined CNN-LSTM network is used to address both the spatial and temporal features of battery data for accurate and robust battery SOC estimation. Specifically, the CNN is used to extract spatial features from the dataset, and the LSTM [15] is used to define relationships between current SOC and historical inputs.

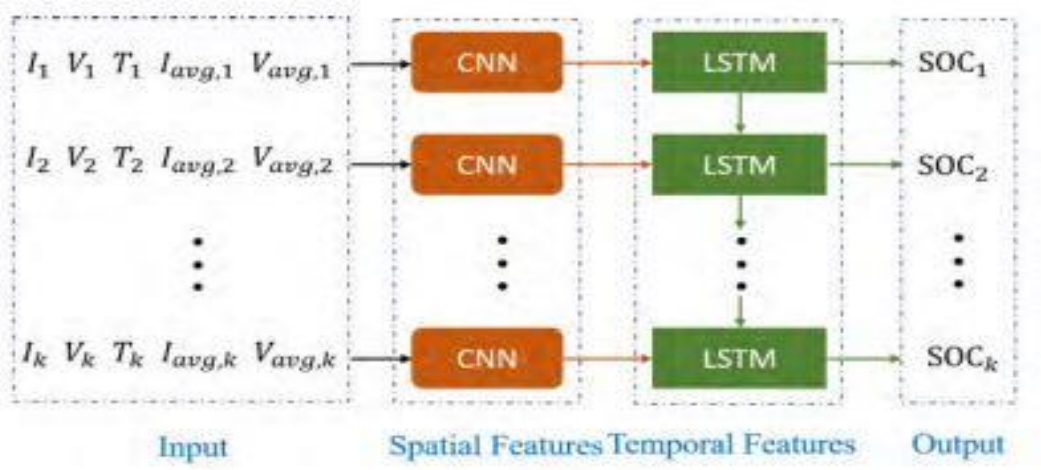

Figure 5.8 Architecture of the combined CNN-LSTM network

The first layer is an input layer, where battery variables including current I, voltage V, temperature T, average current Iavg, and average voltage Vavg are fed into the network. Next is the convolutional layer with six filters of length three is built to extract the spatial features of battery input parameters. Then an LSTM [16] layer is added to learn the temporal features of battery dynamic parameter relations. Finally, a fully connected layer is used as a regression layer to numerically evaluate the final SoC estimation.

The overall loss function for the training process, the RMSE and MAE for the testing process, and all the hidden variable parameters are the same as 5.3.2.

Table 5.2 RMSEs and MAEs of SOC estimation under varying initial states.

Initial SoC	RMSE (%)	MAE (%)
100	0.54	0.41
80	1.35	0.87
60	0.92	0.48
40	1.38	0.53
20	0.58	0.33

5.4 RESULTS

In order to verify the feasibility of above models, the models were built in Python to verify the accuracy of the experiment.

For EKF, input variables were obtained from synthesized data, which includes: time, current, voltage and discharge capacity. The PNGV driving cycle is selected to verify the accuracy of EKF, and the absolute error is used to evaluate the experimental accuracy.

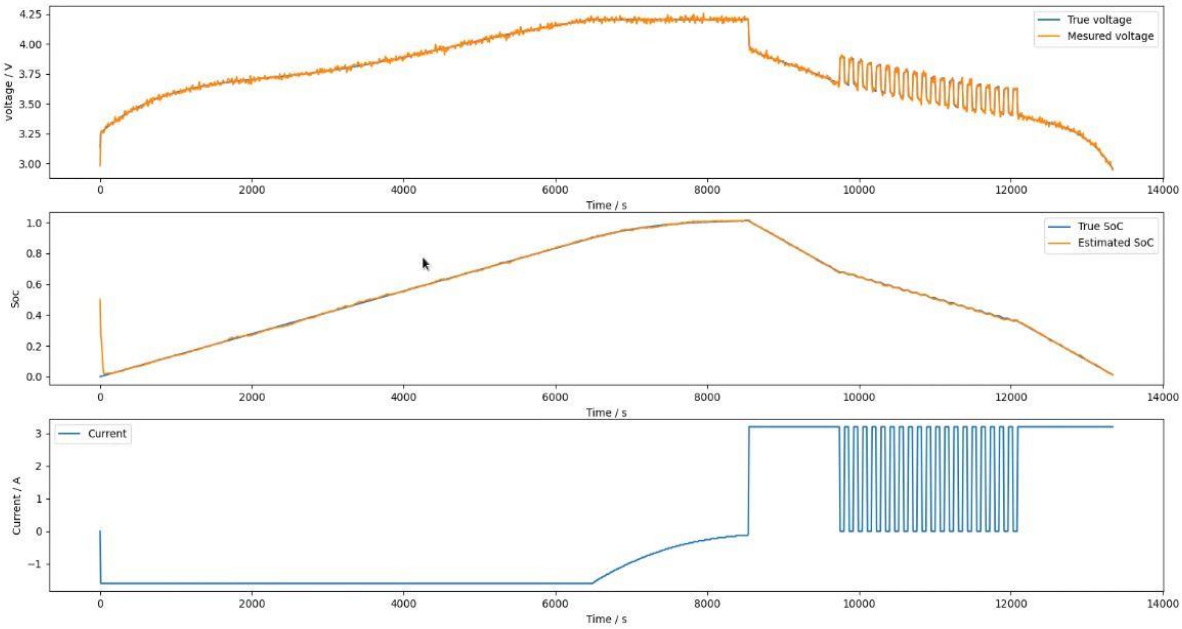

Figure 5.9 (a) The input voltage curve over time (b) The curve of SoC true value and the estimated value (c) The input current over time

For DNN, the discharge data for all 164 cycles and 11,345 sample points from battery No.05 from NASA Ames Prognostics Center of Excellence (PCoE) database were employed. The result is considered to be a long-term SoC estimation of the battery.

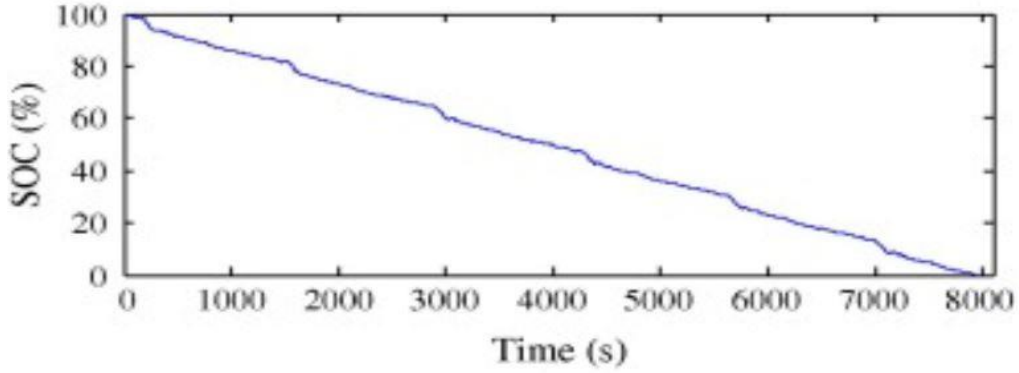

Figure 5.10 The curve of estimated SoC for DNN

The combined CNN-LSTM network is trained with data collected from the simulation using PNGV driving cycle. The input of the network is $x_k = [I_k, V_k, T_k, I_{avg,k}, V_{avg,k}]$, while the output is the corresponding SOC estimation, namely $y_k = [SOC_k]$.

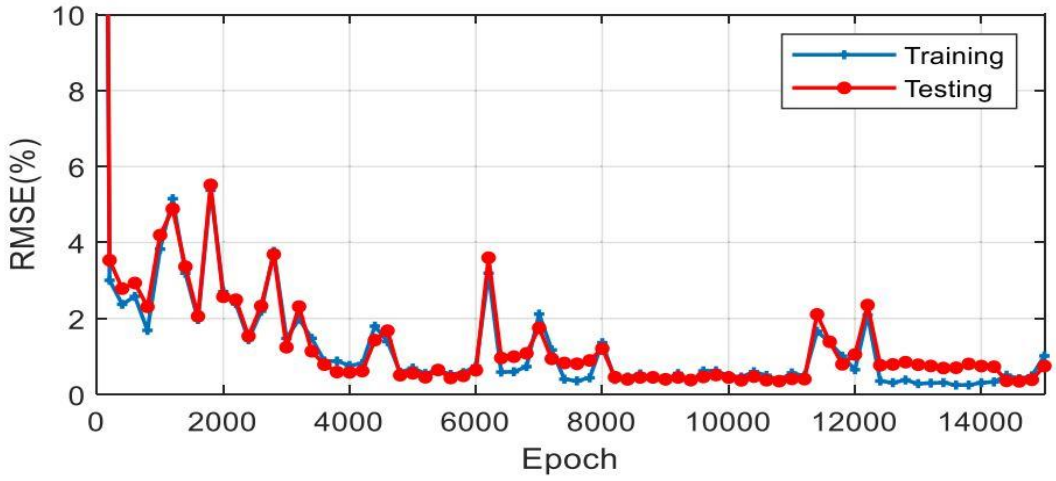

Figure 5.11 RMSEs of the training and testing performance with varying epoch

The SoC Estimation using combined CNN-LSTM network has lowest experimental RMSE value and hence, most efficient network for deployment in the electric vehicle system.

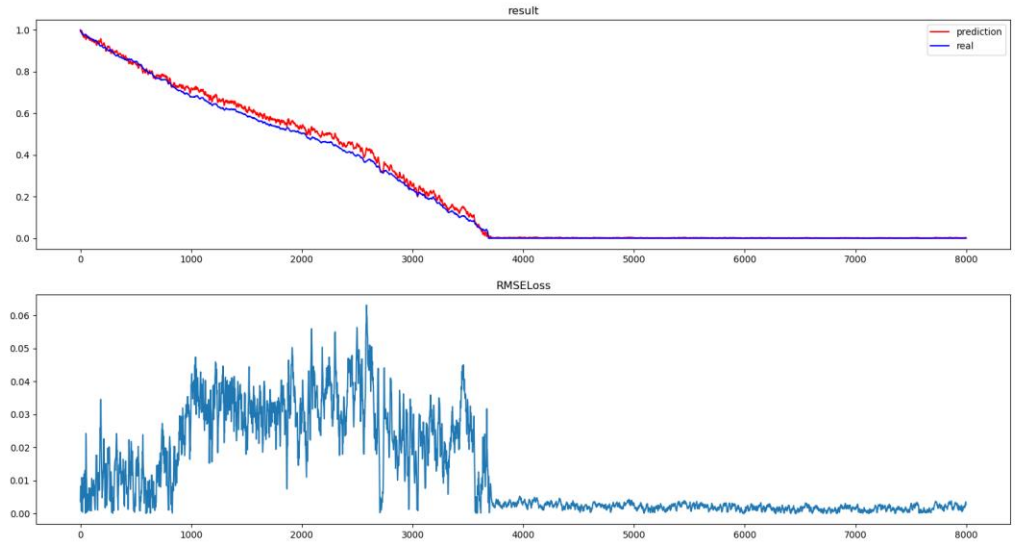

Figure 5.12 (a) The curve of SoC true value and the estimated value (b) The RMSE value with time

CHAPTER VI

Vehicle Dynamics Modelling

Need for modelling

The realization of an electrical vehicle becomes a major factor to test the prediction of the battery and validation of the algorithms wherein the results of prediction have the minimum errors.

The realization of the vehicle will take account of not only the electrical but also the mechanical, aerodynamic and control elements of each and every aspect related to the electrical vehicle.

6.1 Structure of vehicle modelling

The structure of vehicle modelling through Simulink will have six components to realize the vehicle components and control of individual components.

6.1.1 Motor Controller component

Controller plays a pivotal role in maintaining a certain speed and to check if there isn't any sudden inrush current in the motor and also acts as a generator as it works on the principle of regenerative braking.

Here the motor control consists of the reference voltage and actual voltage with a PI controller and a limiter.

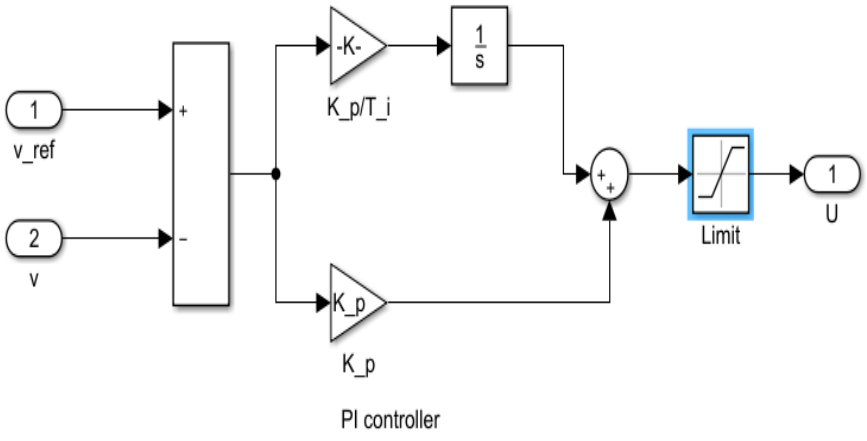

(a)

(b)

Fig 6.1 - (a) The control network of the motor controller, (b) Motor controller unit

6.1.2 Electric motor

Electric motor used here is an induction type of motor hence the motor inputs have two blocks connected to them as in the simulation.

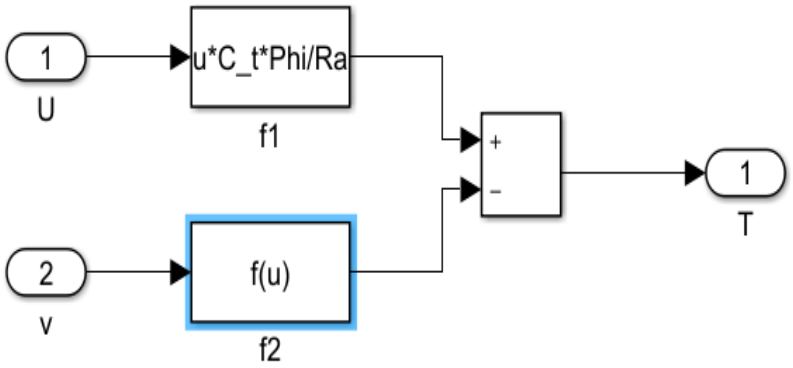

(a)

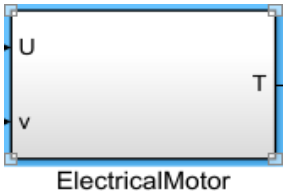

(b)

Fig 6.2 - (a) Electric motor internal blocks, (b) Electric motor block

6.1.3 Kinetic Component

The kinetic component of EV plays a major role in getting access to the simulation of the vehicle's inner situation under different working states which involve the variation of slope and velocity and also figure out the specific power needed from the battery to support the vehicle's work.

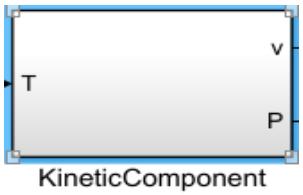

(a)

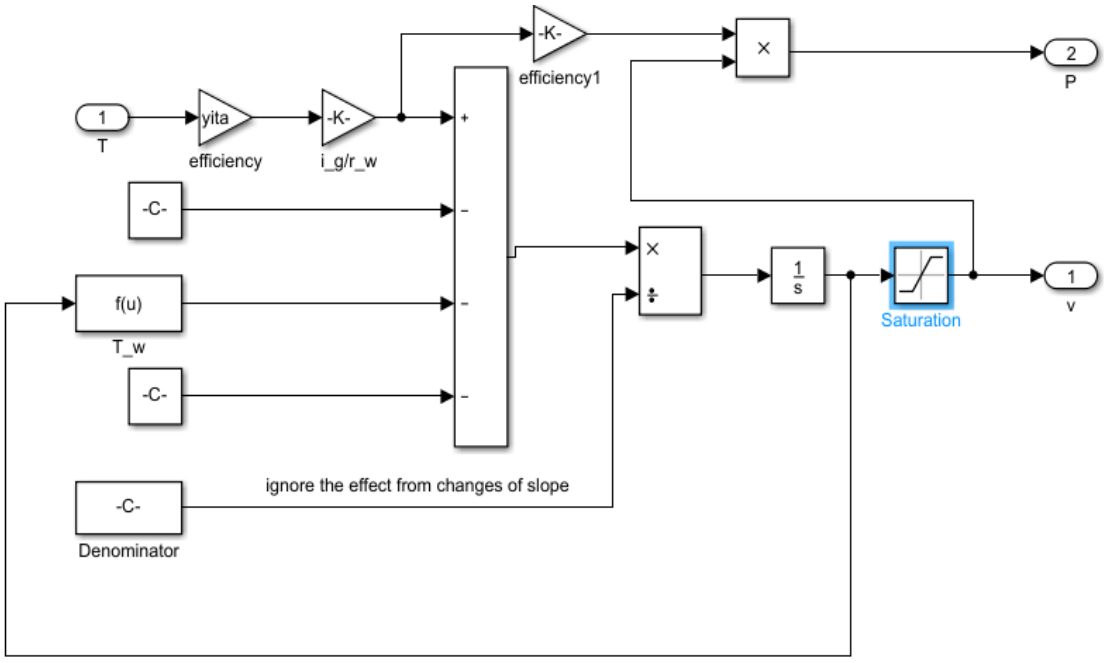

(b)

Fig - 6.3 - (a) Kinetic control block, (b) Internal circuitry of kinetic control block

6.1.4 Battery model

The battery model and control as simulated has been discussed in the previous section and this model has some additional controls given below.

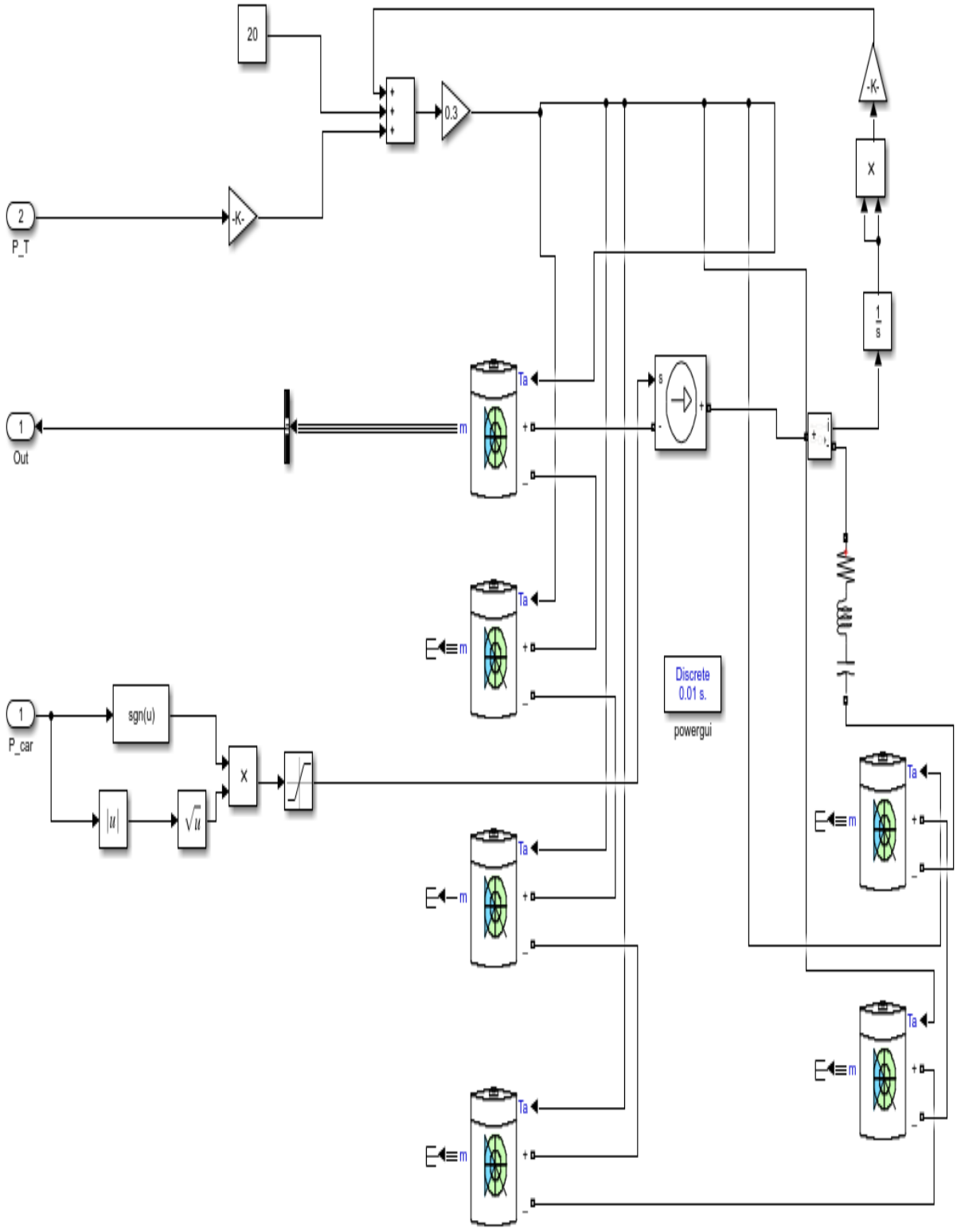

Fig 6.4 - Battery model internal structure

6.1.5 PNGV battery model

The PNGV equivalent battery model [7] is created by analyzing the machine learning algorithms and hence simulating it with the integrators and differentiators to yield an output of predicted SoC using the parameters and a block of updated SoC.

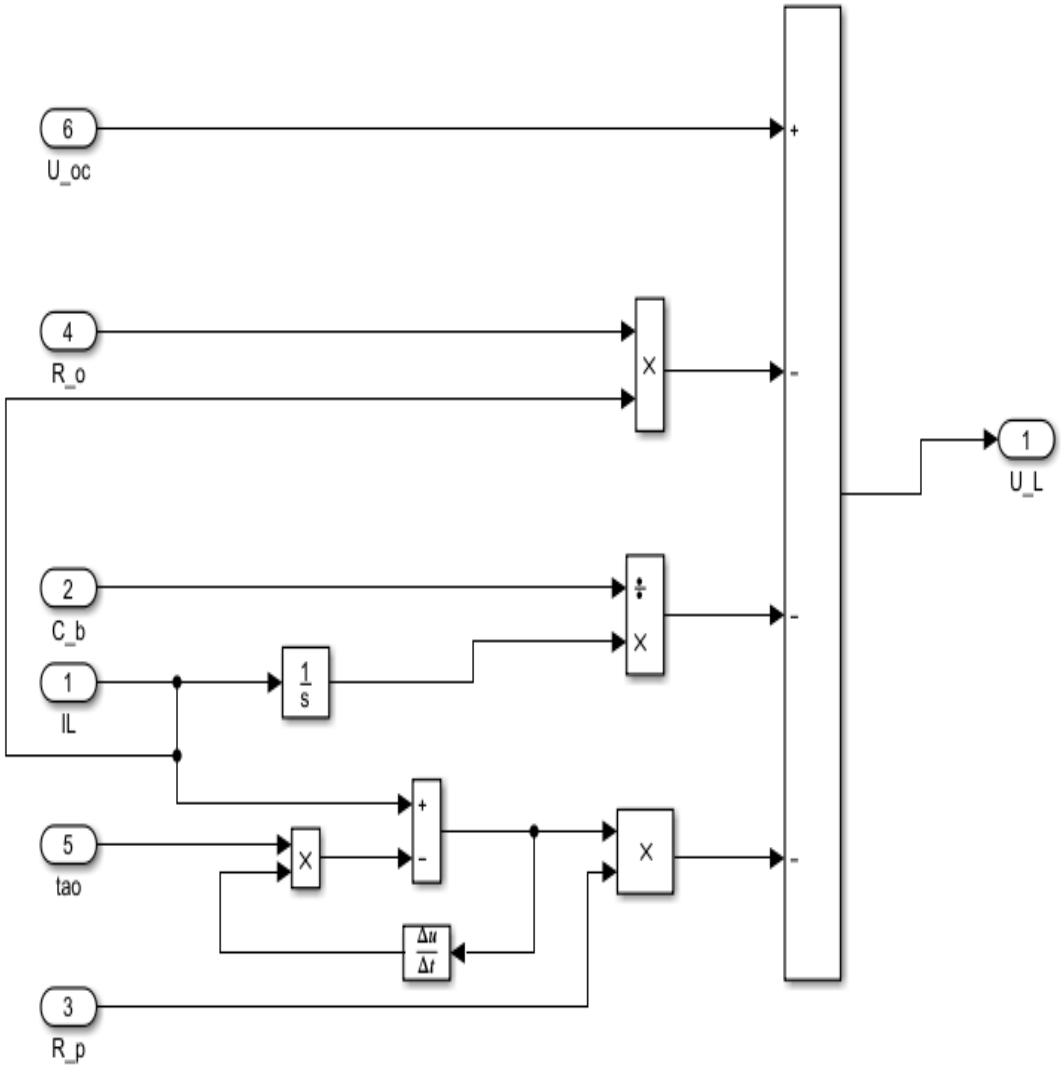

Fig 6.5 - PNGV battery model

6.1.6 Complete Structure

The complete simulation file consists of the motor controller, electric motor, kinetic control model, battery model, power efficiency model, discharge model and the main PNGV battery which yields the prediction of SoC

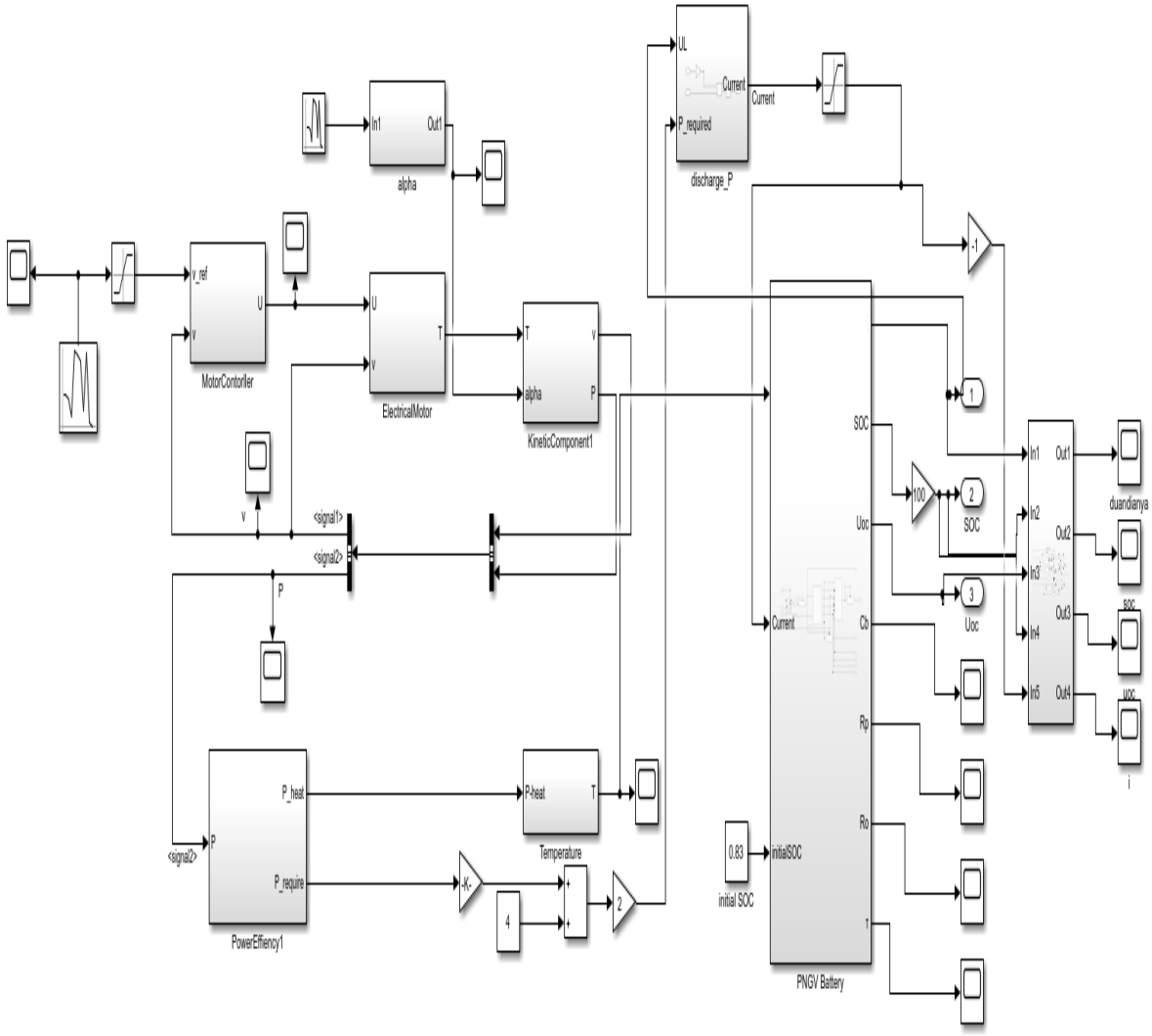

Fig 6.6 - Complete structure of electric vehicle assembly

6.2 Results

6.2.1 Motor voltage V/s Time

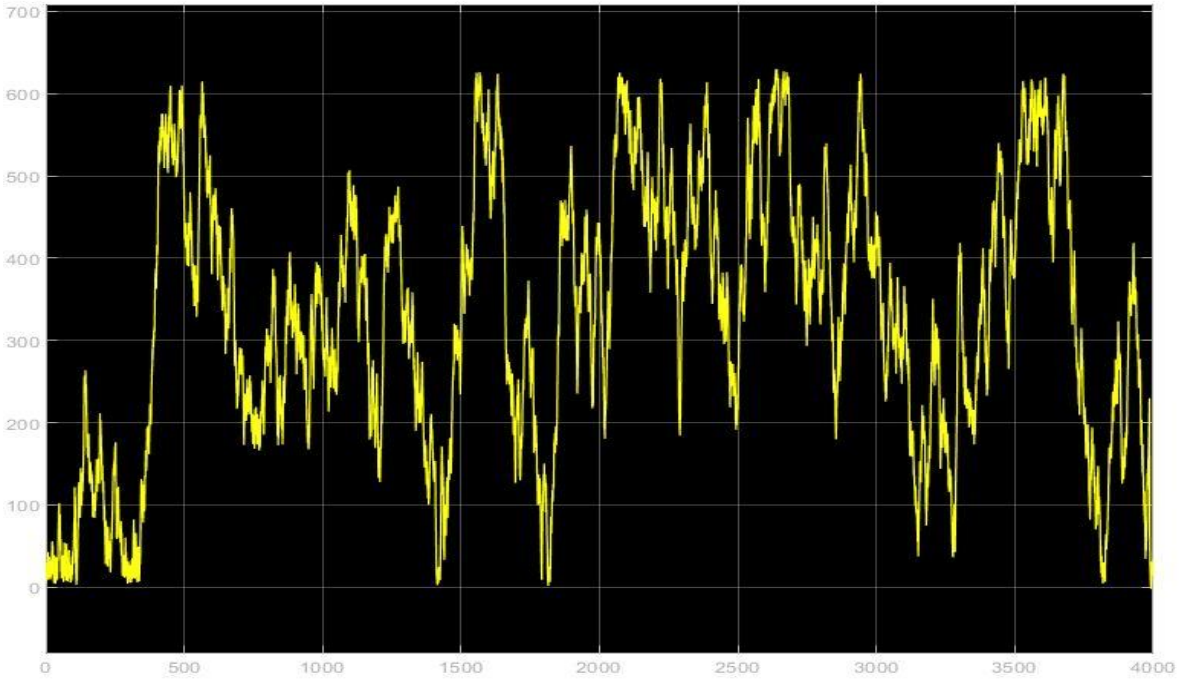

Fig 6.7 - Graph of motor voltage(V) V/s time(s)

6.2.2 Motor Torque V/s Time

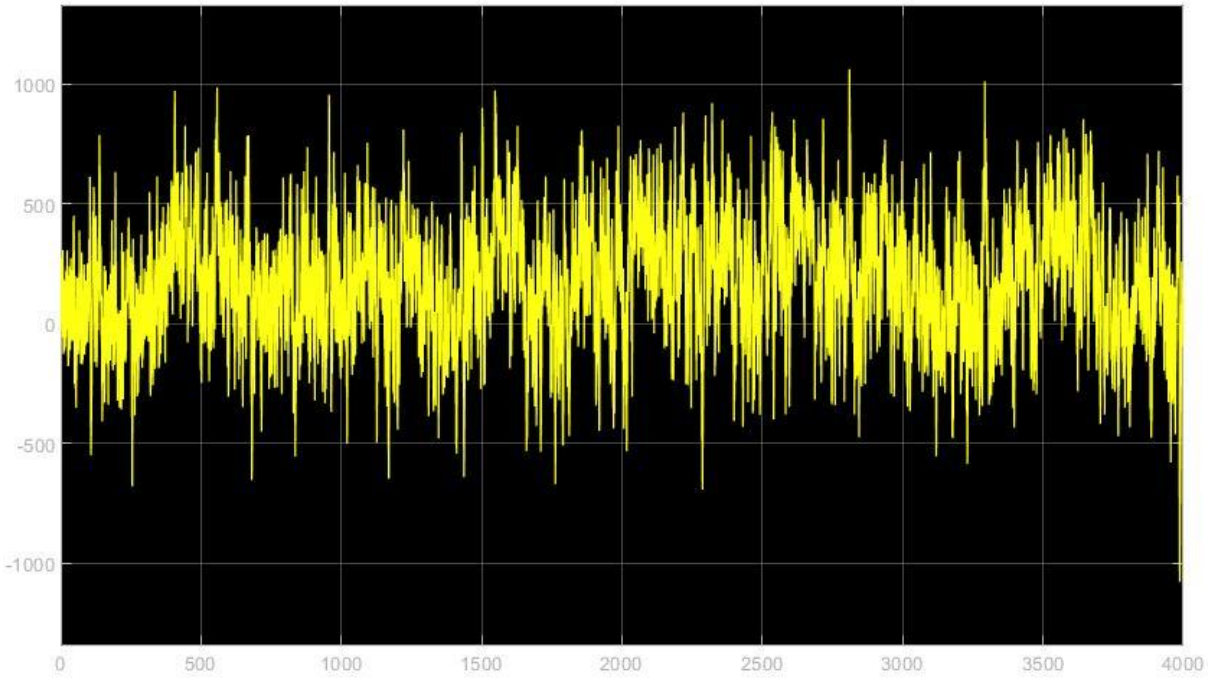

Fig 6.8 - Graph of motor torque(N-m) V/s time(s)

6.2.3 Actual Speed V/s Time

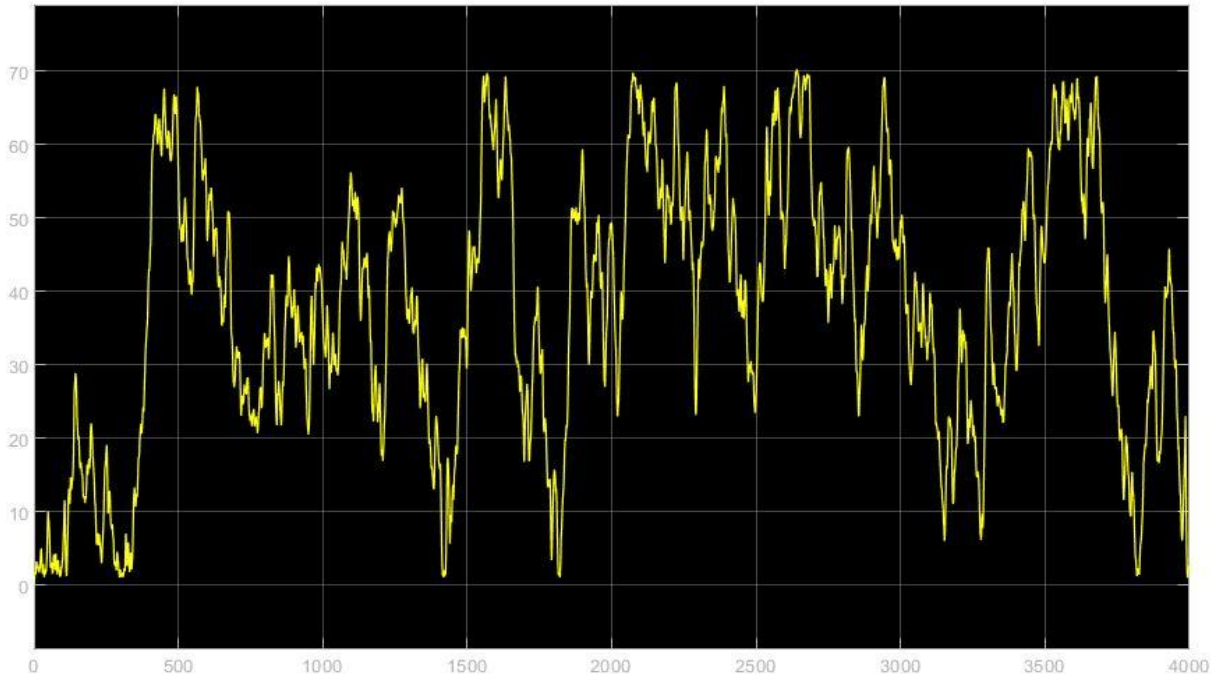

Fig 6.9 - Graph of speed of vehicle(m/s) V/s time(s)

6.2.4 Motor Power V/s Time

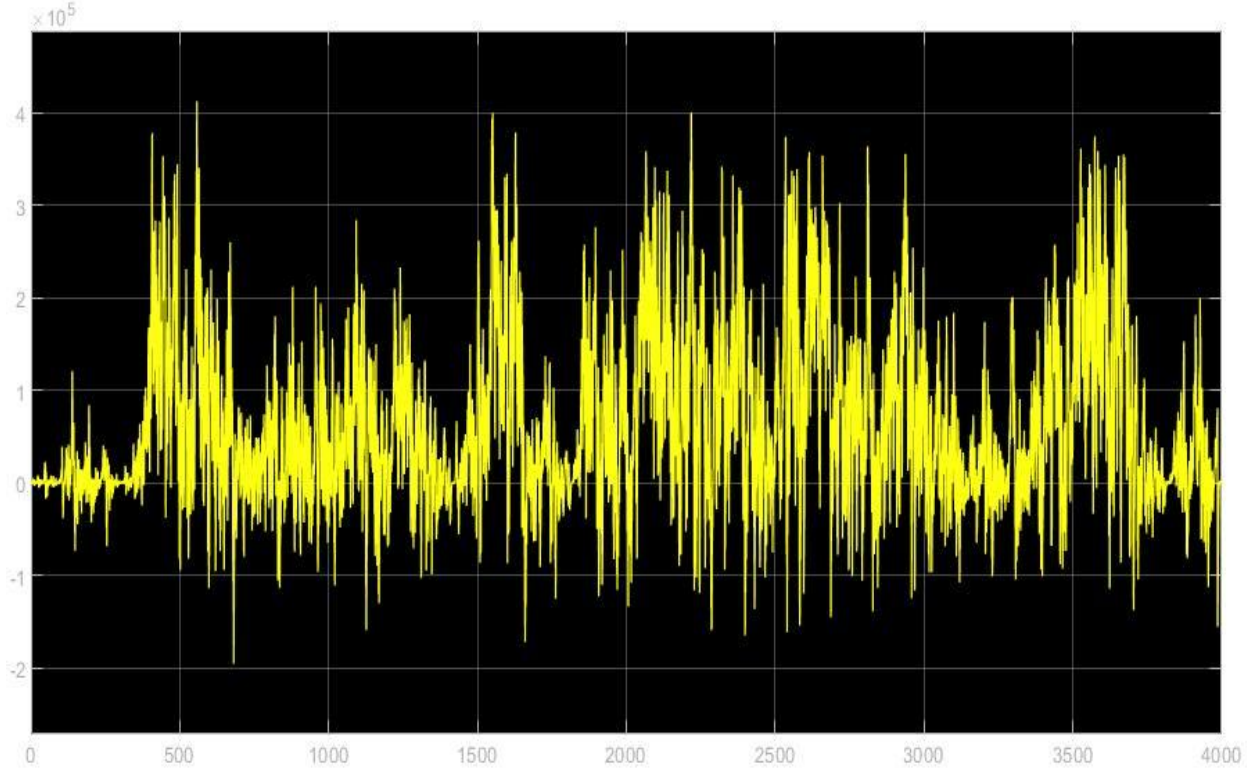

Fig 6.10 - Graph of motor power(W) V/s time(s)

6.2.5 Maximum capacity (Ah) V/s Time

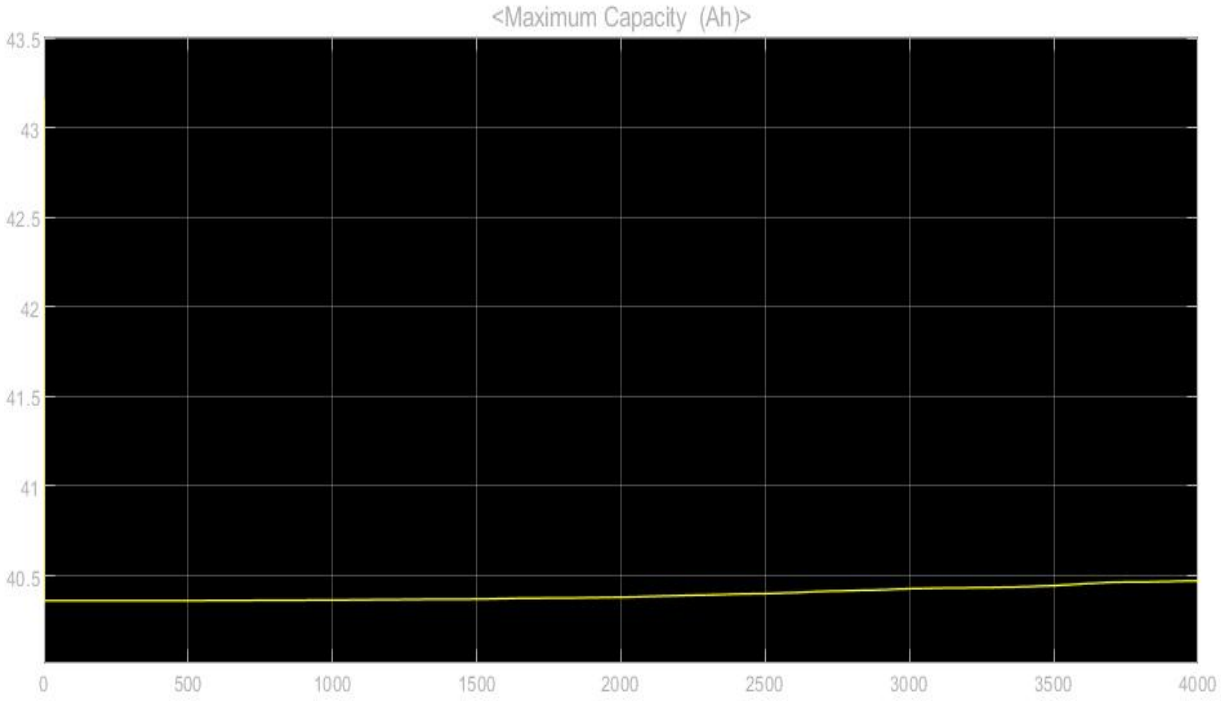

Fig 6.11 - Graph of maximum capacity (Ah) V/s time(s)

6.2.6 Current(A) V/s Time

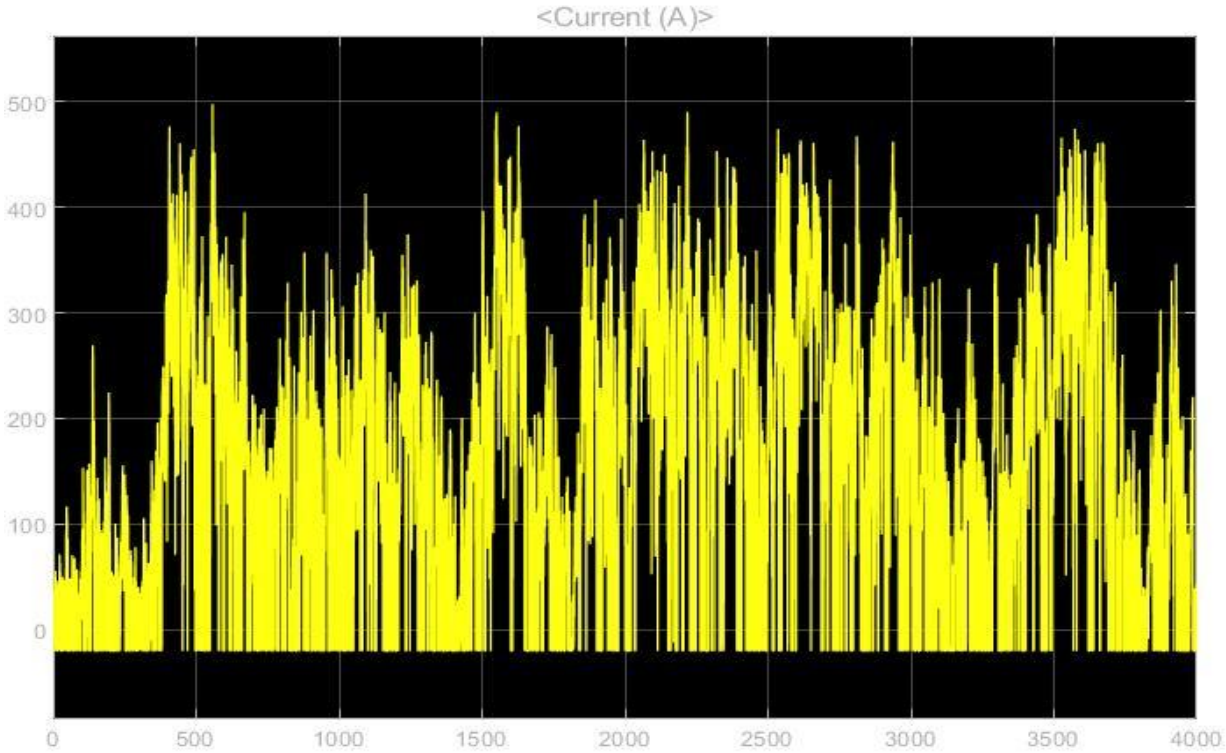

Fig 6.12 - Graph of current(A) V/s time(s)

6.2.7 Voltage(V) V/s Time

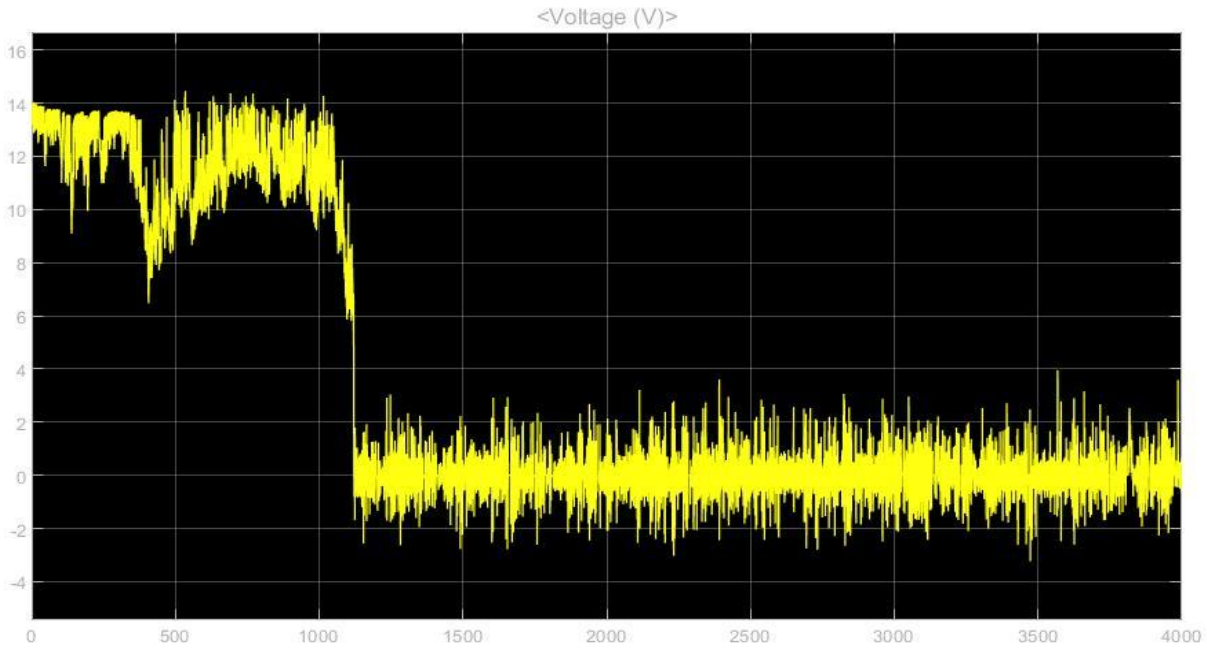

Fig 6.13 - Graph of battery voltage(V) V/s time(s)

6.2.8 SoC V/s Time

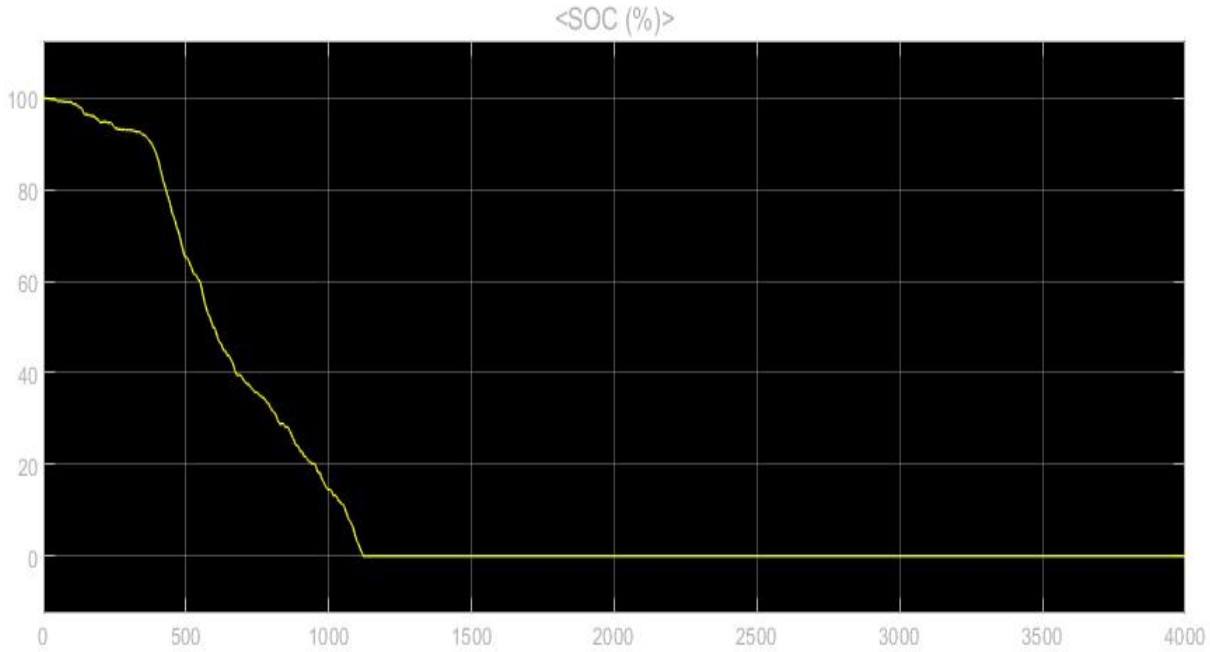

Fig 6.14 - Graph of SoC of battery (%) V/s time(s)

6.2.9 Temperature V/s Time

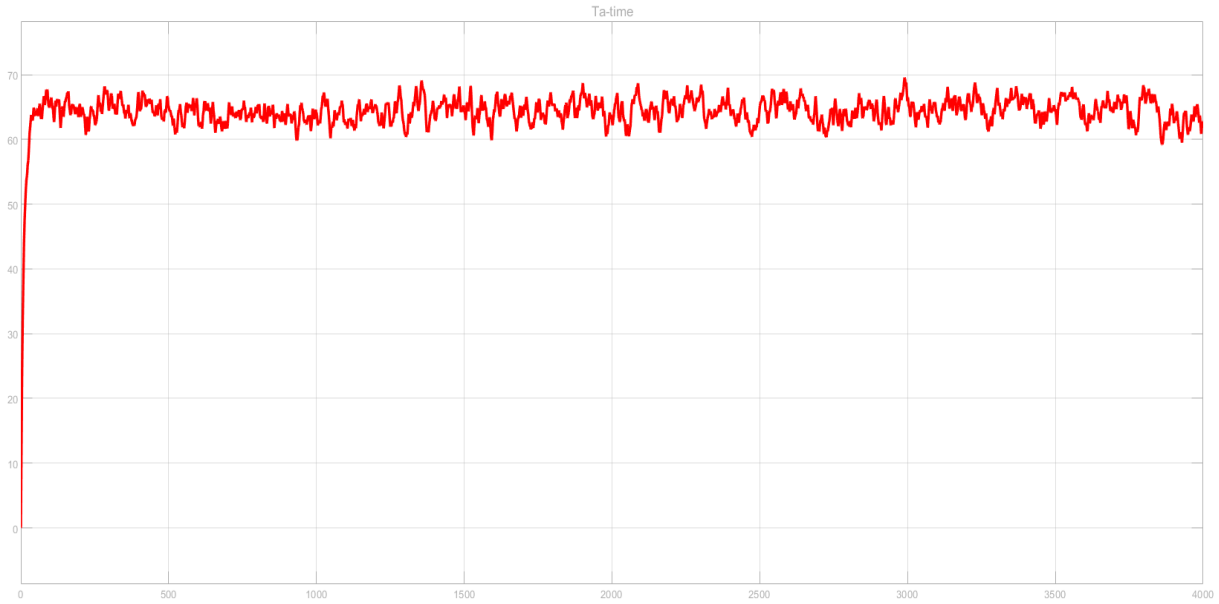

Fig 6.15 - Graph of cell temperature(degrees) V/s time(s)

6.3 Summary of Results

From the results we can observe that the discharging of the battery happens just at a time close to 1100 sec which has brought a dip of zero voltage which makes the SoC of the battery to zero and hence the battery is in a halted stage. The simulation shows a trend which is very near to the original dynamics of a vehicle.

Conclusion

In this thesis the construction of the model and the task of SoC estimation for the battery system in the electric vehicles are demonstrated. We have implemented and tested the various algorithms required in the SoC estimation model in a real-world dynamic environment.

Further a study pertaining to the advanced algorithms of SoC estimation was undertaken which consisted of simulating an electric vehicle assembly consisting of motor controller, kinetic component, power efficiency component and the battery module.

We aim to create an autonomous SoC estimator robust enough to operate accurately in dynamic environments. This would solve the problem of overcharging, over discharging, optimizing the battery performance and increasing its life cycle. This also helps the consumer of the electric vehicle to plan their journey depending on the estimate of SoC with the distance travelled.

Future Scope

1. Development of more optimized and unique models to improve the efficiency and accuracy.

2. Continue to simulate the PNGV and second-order RC models;

3. Try to use the joint estimation method in the literature to obtain SOC, SOH, and SOF at the same time;

4. Continue to consider the impact of temperature on the internal battery.

5. Development of a generalized model for multiple driving behaviors on different terrains.

References

[1] M.A. Hannan, M.S.H. Lipu, A. Hussain, A. Mohamed, A review of lithium-ion battery state of charge estimation and management system in electric vehicle applications: Challenges and recommendations, Renewable and Sustainable Energy Reviews, Volume 78, 2017, Pages 834-854, ISSN 1364-0321.

[2] Chang, Wen-Yeau. (2013). The State of Charge Estimating Methods for Battery: A Review. ISRN Applied Mathematics. 2013.

[3] A. Gensler, J. Henze, B. Sick and N. Raabe, "Deep Learning for solar power forecasting — An approach using AutoEncoder and LSTM Neural Networks," 2016 IEEE International Conference on Systems, Man, and Cybernetics (SMC), Budapest, Hungary, 2016, pp.

[4] S. Hochreiter and J. Schmidhuber, ‘‘Long short-term memory,’’ Neural Comput., vol. 9, no. 8, pp. 1735–1780, 1997.

[5] Huaizhi Wang, Zhenxing Lei, Xian Zhang, Bin Zhou, Jianchun Peng, A review of deep learning for renewable energy forecasting, Energy Conversion and Management, Volume 198, 2019, 111799, ISSN 0196-8904

[6] B. Saha and K. Goebel (2007). "Battery Data Set", NASA Ames Prognostics Data Repository, NASA Ames Research Center, Moffett Field, CA

[7] Hinton, G.E.; Salakhutdinov, R.R. Reducing the dimensionality of data with neural networks. Science 2006, 313, 504–507.

[8] G. L. Plett, ‘‘Sigma-point Kalman filtering for battery management systems of LiPB-based HEV battery packs: Part 1: Introduction and state estimation,’’ J. Power Sour., vol. 161, no. 2, pp. 1356–1368, 2006.

[9] C. Huang, Z. Wang, Z. Zhao, L. Wang, C. S. Lai, and D. Wang, ‘‘Robustness evaluation of extended and unscented Kalman filter for battery state of charge estimation,’’ IEEE Access, vol. 6, pp. 27617–27628, 2018.

[10] G. L. Plett, ‘‘Extended Kalman filtering for battery management systems of LiPB-based HEV battery packs: Part 1. Background,’’ J. Power Sour., vol. 134, no. 12, pp. 252–261, 2004.

[11] Hegazy, T.; Fazio, P.; Moselhi, O. Developing practical neural network applications

using back-propagation. Comput. Aided Civ. Infrastruct. Eng. 1994, 9, 145–159.

[12] E. Chemali, P. J. Kollmeyer, M. Preindl, and A. Emadi, ‘‘State-of-charge estimation of Li-ion batteries using deep neural networks: A machine learning approach,’’ J. Power Sources, vol. 400, pp. 242–255, Oct. 2018.

[13] Srivastava, N.; Hinton, G.; Krizhevsky, A.; Sutskever, I.; Salakhutdinov, R. Dropout: A simple way to prevent neural networks from overfitting. J. Mach. Learn. Res. 2014, 15, 1929–1958.

[14] D. P. Kingma and J. Ba, ‘‘Adam: A method for stochastic optimization,’’ Dec. 2014, arXiv:1412.6980.

[15] E. Chemali, P. J. Kollmeyer, M. Preindl, R. Ahmed and A. Emadi, "Long Short-Term Memory Networks for Accurate State-of-Charge Estimation of Li-ion Batteries," in IEEE Transactions on Industrial Electronics, vol. 65, no. 8, pp. 6730-6739, Aug. 2018.

[16] F. Yang, X. Song, F. Xu, and K.-L. Tsui, ‘‘State-of-charge estimation of lithium-ion batteries via long short-term memory network,’’ IEEE Access, vol. 7, pp. 53792–53799, 2019.

[17] X. Liu, W. Li and A. Zhou, "PNGV Equivalent Circuit Model and SOC Estimation Algorithm for Lithium Battery Pack Adopted in AGV Vehicle," in IEEE Access, vol. 6, pp. 23639-23647, 2018.